CHARLES UNIVERSITY

Faculty of Pharmacy in Hradec Králové

Department of Pharmacology and Toxicology

UNIVERSITY OF LJUBLJANA

Faculty of Pharmacy

The Chair of Clinical Biochemistry

Analysis of the molecular pathways and interactome of FUBP3

Diploma thesis

Supervisors:

Assist. Prof. Eduard Jirkovský, PharmD, PhD

Assist. Prof. Nika M. Lovšin, M. Chem., PhD

Ljubljana & Hradec Králové 2023

David Brychta

Hereby I declare, this thesis is my original work. All literature and other sources I used while processing are listed in the bibliography and properly cited. To my knowledge, this thesis has not been submitted for obtaining the same or any other degree.

Hradec Králové 17.03.2023 David Brychta

Acknowledgements

My great acknowledgment goes to Assist. Prof. Eduard Jirkovský, PharmD, PhD, for guiding me through the process of writing the thesis, for proofreading it, and for his insightful counsel.

I would like to express my sincere gratitude to Assist. Prof. Nika Lovšin, M. Chem., PhD, who welcomed me to join her research team during my Erasmus year in Ljubljana, guided my lab work through the pandemic times, and provided me with much valuable advice.

Last but not least, I would like to thank my family and friends for their unwavering support.

Abstract

Charles University, Faculty of Pharmacy in Hradec Králové
Department of Pharmacology and Toxicology
Candidate: David Brychta
Supervisor: Assist. Prof. Eduard Jirkovský, PharmD, PhD.; Assist. Prof. Nika M. Lovšin, M.Chem., PhD
Title of Diploma Thesis: Analysis of the molecular pathways and interactome of FUBP3

The far upstream element-binding protein 3 (FUBP3) has been recognized by genome-wide association studies to be associated with a higher risk of osteoporotic fracture. The knowledge about this protein and its role in bone biology is quite limited, though. Therefore, we aimed to broaden the horizons and created an overview of FUBP3 protein-protein interactors and possible pathway involvement.

The interacting proteins were gathered across multiple databases. Their association with osteoporosis (OP) and bone mineral density (BMD) was assessed using an online tool - OpenTargets Platform. Twelve hits associated with either were then used for qPCR analysis to investigate the influence of FUBP3 knockout. Among FUBP3 interactors were also proteins of cytosolic membraneless organelles – stress granules (SG). Stress conditions were induced and co-localization of SG markers PABPC1 and G3BP1 was carried out using immunostaining and fluorescence microscopy.

We were able to identify 75 protein interactors associated with either OP or BMD, out of which 8 were chosen as targets of interest for qPCR analysis. We report Osteocalcin, Collagen type I alpha 1 chain, and Transmembrane protein 64 to be differentially expressed in FUBP3 knockout human osteosarcoma cells. We were also able to successfully co-localize both SG markers with FUBP3 and conclude that it is a part of the stress granule proteome. Our results shall serve as a starting point for further studies of FUBP3's role in bone biology.

Abstrakt

Univerzita Karlova, Farmaceutická fakulta v Hradci Králové
Katedra farmakologie a toxikologie
Kandidát: David Brychta
Školitel: PharmDr. Eduard Jirkovský, PhD.; Nika M. Lovšin, M. Chem., PhD
Název diplomové práce: Analýza molekulárních drah a interaktomu FUBP3

Far upstream element-binding protein 3 (FUBP3) byl pangenomickými asociačními studiemi spojován s vyšším rizikem osteoporotických fraktur. Znalosti o tomto proteinu a jeho roli v biologii kostí jsou však značně omezené. Proto jsme si vytyčili za cíl rozšířit obzory a vytvořit přehled proteinů interagujících s FUBP3 a zmapovat možné zapojení do buněčných drah.

Interagující proteiny byly shromážděny z různých databázích. Jejich asociace s osteoporózou (OP) a kostní minerální hustotou (BMD) byla hodnocena pomocí online nástroje – OpenTargets Platform. Několik z nich pak bylo použito pro qPCR analýzu k posouzení vlivu knockoutu FUBP3. Mezi interaktory FUBP3 se objevovaly i proteiny cytosolických bezmembránových organel – stresových granulí (SG). Vytvořili jsme stresové podmínky a byla provedena co-lokalizace SG markerů PABPC1 a G3BP1 pomocí imunobarvení a fluorescenční mikroskopie.

Podařilo se nám identifikovat 75 proteinů interagujících s FUBP3 spojených buď s OP nebo BMD, z nichž 8 bylo vybráno pro qPCR analýzu. Zjistili jsme, že osteocalcin, collagen type I alpha 1 chain a transmembrane protein 64 jsou odlišně exprimovány v buňkách lidského osteosarkomu s knockoutem FUBP3. Podařilo se nám také úspěšně co-lokalizovat oba SG markery s FUBP3 a docházíme k závěru, že je součástí proteomu stresových granulí. Naše výsledky mohou sloužit jako výchozí bod pro další studium role FUBP3 v biologii kostí.

Table of contents

1. List of abbreviations

A549 - human lung (carcinoma) cell line

AF - Alexa Fluor

APP – Amyloid-beta precursor protein

BMD - bone mineral density

BM-MSC - bone marrow-derived mesenchymal stem cell

BSA - bovine serum albumin

cDNA - complementary DNA

COL1A1 – collagen type I alpha 1

DMEM - Dulbecco's Modified Eagle Medium

FBS - fetal bovine serum

FGF – Fibroblast growth factor

FUBP - far upstream element-binding protein

Fw - forward

G3BP1 - ras GTPase-activating protein-binding protein 1

GFP - green fluorescent protein

GWAS - genome-wide association study

HeLa - human cervical cancer cell line

HOS - human osteosarcoma cell line

ko - knockout

MG-63 - human osteosarcoma cell line

OC - osteocalcin

OP - osteoporosis

pAb - primary antibody

PABPC1 - poly(A) binding protein cytoplasmic 1

PBS - Phosphate-buffered saline

PFA - paraformaldehyde

PTEN - phosphatidylinositol 3,4,5-trisphosphate 3-phosphatase and dual-specificity protein phosphatase

qPCR - quantitative polymerase chain reaction

Rev - reverse

RHOA - transforming protein RhoA

RT - room temperature

sAb - secondary antibody

SG - stress granule

SYNCRIP - heterogeneous nuclear ribonucleoprotein Q

TMEM64 - transmembrane protein 64

wt - wild type

2. Introduction

FUBP3 (Far Upstream Element Binding Protein 3) is a multifunctional protein that plays a role in the regulation of gene expression. It is a DNA- and RNA-binding protein that binds to the far upstream element (FUSE) of the c-myc oncogene and regulates its expression. In addition to its role in transcriptional regulation, FUBP3 has been shown to be involved in several cellular processes, including DNA replication, splicing, and mRNA translation.

Recent studies have suggested that FUBP3 is also involved in stress response. In response to cellular stress, such as heat shock or oxidative stress, stress granules play a crucial role in the regulation of mRNA translation during stress and are essential for cell survival under stress conditions.

Furthermore, FUBP3 has been identified as a target of interest in osteoporosis. Osteoporosis is a disease characterized by reduced bone density and increased risk of fractures, and it affects millions of people worldwide. Recent studies have suggested that dysregulation of gene expression, including FUBP3, may be involved in the pathogenesis.

Understanding the mechanisms underlying FUBP3 localization to stress granules and its role in osteoporosis requires a detailed analysis of the FUBP3 interactome. FUBP3 interacts with various proteins involved in various cellular processes, and identifying these interaction partners can provide insight into the diverse functions of FUBP3.

In conclusion, studying the co-localization of FUBP3 with stress granule proteins and the FUBP3 interactome is crucial for understanding the role of this multifunctional protein in stress response pathways and osteoporosis.

3. Theoretical part

3.1. Bone biology

The bone tissue serves several purposes in the human body, such as movement facilitation, protection and support of soft tissue, calcium and phosphate storage, and holding of bone marrow. The bone is composed of extracellular matrix, mineralized tissue, and several specialized cell types, including osteoblasts, osteoclasts, and osteocytes, which work together to maintain bone structure and function. Although appearing inert, the bone tissue is highly dynamic, continuously undergoing resorption and neoformation (Florencio-Silva et al., 2015).

Osteoblasts are responsible for bone neoformation, while osteoclasts are the bone resorption-responsible cells (Teitelbaum & Ross, 2003). Osteocytes, the most abundant cell type in bone, play a crucial role in bone homeostasis. Together with bone-lining cells, these are the four types of cells present in the bone tissue (Florencio-Silva et al., 2015).

3.1.1. Bone metabolism

The process of regulated old bone resorption and replacement is called bone remodelling and it is highly compound. The bone undergoes remodelling without overall change in its three-dimensional shape. For remodelling, the necessary coupling of osteoblastic and osteoclastic functions into a defined remodelling unit needs to take place (Buck & Dumanian, 2012).

Osteoblasts are the key cells involved in bone formation – ossification. They synthesise and secrete the organic matrix of bone, mainly composed of type I collagen, osteocalcin, and other non-collagenous proteins. Osteoblasts also produce alkaline phosphatase, an enzyme that is essential for the mineralization of bone. Osteoblasts originate from mesenchymal stem cells – a common starting point of muscle, fat and cartilage lineages (Rodan, 1992).

The master transcriptional regulator for osteoblast lineage is Runx2 (also known as Cbfa1). Once activated by Runx2, preosteoblasts undergo 3-step differentiation into osteoblasts, with each stage defined by the expression of specific markers. (Figure 1) The major regulatory pathways involved in Runx2 regulation are the Wnt and Notch pathways, thus also regulating osteoblastic differentiation (Rutkovskiy et al., 2016).

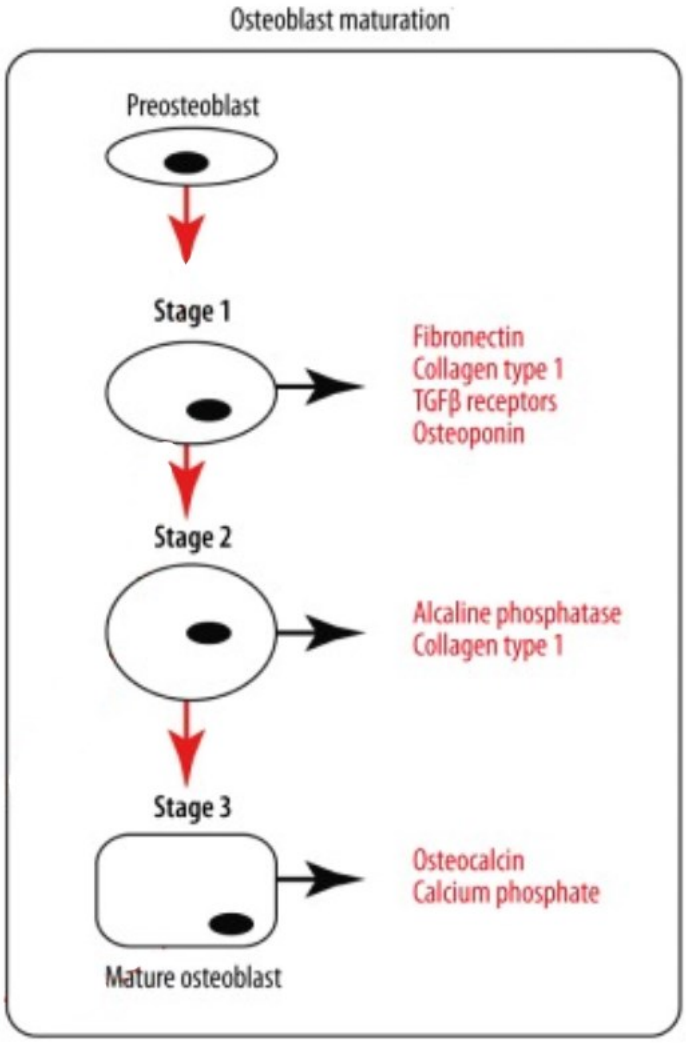

Figure 1*: Osteoblast maturation from preosteoblast to a mature osteoblast; markers characteristic for each stage of development are written in red; picture adapted from Rutkovskiy et al., 2016*

The balance between Wnt and Notch signalling systems is crucial to natural osteoblastogenesis. Wnt pathway activation plays in favour of osteoblast differentiation, while Notch signalling impairs osteoblastogenesis (Canalis, 2008). The Wnt ligands, engaging membrane receptors, stimulate intracellular pathways either dependent or independent of β-catenin. β-catenin interacts in a complex with glycogen synthase kinase 3β (GSK3β), Axin and adenomatous polyposis coli, marking it for degradation. The β-catenin dependent Wnt signalling leads to inhibition of GSK3β, therefore β-catenin is stabilized and saved from degradation. Osteoblast differentiation requires the presence of β-catenin, specifically for the progression from the RUNX2+ OSX+ stage to mature osteoblasts (Long, 2011). Moreover, abnormal Wnt regulation

is linked to various malignancies, aortic valve calcification or extreme bone mass deviations (Johnson & Rajamannan, 2006).

In osteoblasts, the Notch system antagonizes Wnt signalling, decreasing levels and activity of β-catenin by GSK3β-mediated degradation (Canalis, 2008). Additionally, Notch enhances the expression of Runx2 inhibitors Hes1, HeyL and Hey1. Furthermore, Notch was established to maintain osteoblastic progenitors in an undifferentiated stage (Rutkovskiy et al., 2016).

The cells carrying out bone resorption are called osteoclasts (Rodan, 1992). They are, contrary to osteoblasts, terminally differentiated cells, originating from hematopoietic stem cell (HSC) lineage. The most important factors influencing osteoclastic development are macrophage colony-stimulating factor (M-CSF) and receptor activator of nuclear factor κB ligand (RANKL) (Florencio-Silva et al., 2015). M-CSF is central to the proliferation of the osteoclast progenitors, whereas RANKL - binding to RANK - directly contributes to the differentiation process (Datta et al., 2008).

Early differentiation is dependent on PU.1 and microphthalmia-associated transcription factor (MITF) and M-CSF. The early osteoclast precursor, stimulated by RANKL, commits to the osteoclast fate. Signalling molecules included in the process are tumour necrosis factor receptor-associated factor 6 (TRAF6), nuclear factor κB (NFκB), c-Fos and Fra-1. RANKL also binds to osteoprotegerin (OPG) - a protein secreted by the cells of osteoblastic lineage, which acts as a decoy receptor, inhibiting RANKL-induced osteoclastogenesis (Teitelbaum & Ross, 2003). The process is described in Figure 2.

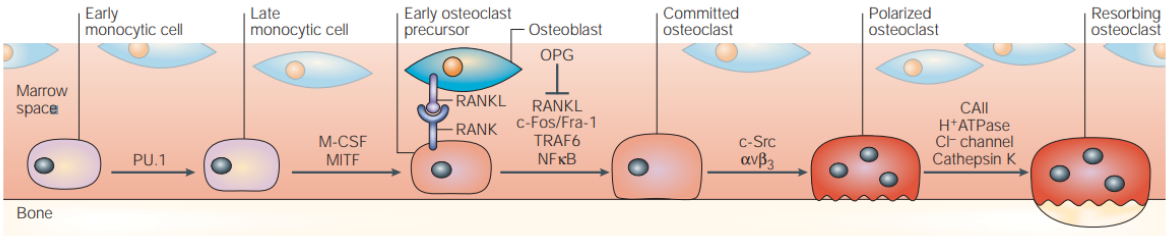

***Figure 2**: Osteoclast development; polarization of the mature osteoclast requires c-Src and the αvβ3 integrin. Once polarized, the osteoclast mobilizes the mineralized component of bone. Bone mobilization is achieved through the acidifying molecules, carbonic anhydrase II (CAII),*

an electrogenic H+ATPase and a charge-coupled Cl– channel; adapted from Teitelbaum & Ross, 2003

Communication between osteoblasts and osteoclasts occurs via cytokines or direct cell contact in various stages of differentiation. The regulation is bidirectional. Besides above mentioned OPG, transmembrane ligand Ephrin2 on osteoclasts and ephrin receptor EphB4 mediate the process. The forward signalling by Eph stimulates osteoblast differentiation by inhibiting RhoA and induces bone formation. In reverse, Ephrin down-regulates c-Fos and NFATc1 expression, inhibiting osteoclast formation. Moreover, EphB4 signalling is known to induce osterix and Runx2. However, the osteoblast-osteoclast cross talk is far more complex and molecules such as semaphorins, lysophosphatidic acid, Fas ligand, d2 isoform of vacuolar ATPase V0 domain and others are involved (Chen et al., 2018).

The basic multicellular unit (BMU) of bone comprises osteoblast, osteoclast and osteocytes. The activity of BMU is regulated by hormones, local factors, cytokines and mechanical forces. Activation of the BMU results in the retraction of the bone lining cells. Osteoclasts are then attracted to the cavity and mature into resorptive multinuclear activated osteoclasts. The underlying bone is digested, followed by the recruitment of osteoblasts to the cavity. The osteoblasts produce osteoid, the basis of new bone tissue. The cycle is finalized by mineralization and differentiation of the osteoblast in either osteocytes or bone-lining cells on the surface (Datta et al., 2008). Imbalance in this process is tied to diseases such as osteoporosis, where bone resorption is predominant (Chen et al., 2018).

3.2. Genetics of osteoporosis

Osteoporosis is a major health issue associated with fractures. The most common fractures are of the hip, spine and wrist. The economic burden of osteoporosis is vast and set to rise by 2050 to 131.5 billion USD annually (Harvey et al., 2010).

The scientific advancement over past decades has brought us to a stage where whole-genome sequencing, as a part of personalized healthcare, might become a routine practice. It is therefore time-worthy to interest ourselves in the genetics of osteoporosis. The advance in mapping the genes related to the disease was made possible by the implementation of genome-wide association studies (GWAS) (Clark & Duncan, 2015). The diagnosis of osteoporosis is focused

on bone mineral density (BMD) evaluation. Osteoporosis is defined as a T-score of 2.5 or lower (t-score is a number of standard deviations from the BMD of a healthy young person) (Kanis, 2002). Bone mineral density is a highly heritable trait with 60-90% of BMD variation being genetically determined (Duncan & Brown, 2010). Besides BMD, other traits such as fracture risk, bone geometry or bone turnover rate are significantly heritable.

Altogether, over 90 loci have been identified through GWAS to be associated with BMD and hundreds more for ultrasound-estimated heel BMD and other bone-related phenotypes (Trajanoska & Rivadeneira, 2019). GWA studies have confirmed seven previously reported genes associated with BMD, namely genes encoding Osteoprotegerin, RANK and RANKL, also LDL receptor-related protein 5 (LRP5), Sclerostin (SOST), Oestrogen Receptor 1, and Parathyroid Hormone. Alongside LRP5 and SOST, novel loci involved in the Wnt pathway have been reported, those are genes for Axin, ß-catenin, Wnt family members, a major Wnt pathway inhibitor Dickkopf-Related Protein 1, an activator of Wnt/ß-catenin signalling R-Spondin3 and others. Genes of importance to ossification code for M-CSF, Myocyte Enhancer Factor 2C, Osteoregulin, Osteopontin, Runx2, Sox6/9 or Osterix. A Ligand for multiple Notch receptors, protein jagged one, has also been reported. However, many BMD loci without evident relation to bone development remain (Hsu & Kiel, 2012).

3.2.1. GWAS recognition of FUBP3

A single nucleotide polymorphism in the locus 9q34.11 has been reported to have a statistically significant effect on femoral BMD by Estrada et al. (2012) in a GWAS meta-analysis. The locus is mapped to the near FUBP3 gene coding for the far-upstream element binding protein 3.

Genome-wide significance of the polymorphism has been further confirmed by another GWAS meta-analysis performed by Trajanoska et al. (2018) not only for BMD but for fracture risk as well. L. Han et al. (2022) suggest that genetic variants causing RNA modification may alter FUBP3 expression, including mRNA levels and protein levels - proposing an insight into the possible involvement of FUBP3 in BMD and osteoporosis pathogenesis. Validation of FUBP3 as an important marker for osteoporosis has been performed by Watts et al. (2020). In FUBP3 knockout mice, short stature, decreased bone mass across vertebrae and femurs, and reduced thickness of cancellous bone have been observed.

3.3. Cellular stress

3.3.1. Stress granules

Every cell is permanently challenged with changing and sometimes stressful conditions such as osmotic stress, temperature fluctuation, or the presence of toxic agents. Therefore, cells evolved many mechanisms to avoid the harmful consequences of stress including global inhibition of translation and formation of stress granules (SGs).

SGs are cytosolic membrane-less entities consisting of stalled pre-initiation complexes with 40S ribosomal subunits and some translation initiation factors, many SG-scaffolding proteins such as G3BPs or TIA-1 or several components of various signalling pathways (Anderson & Kedersha, 2008). The role of SGs is to help protect the stalled transcripts and cellular proteins from the negative influence of stress conditions. If the stress fades away, SGs dissolve and the cell continues with translation, however, if the impact of stress is too extensive, it leads the cell to apoptosis (Pakos-Zebrucka et al., 2016).

The forming of SGs is an active ATP-requiring process called phase separation (Jain et al., 2016). It is induced mainly by translation inhibition caused by the phosphorylation of the translation initiation factor 2 (eIF2) (Kedersha et al., 1999).

Stress conditions and the formation of SGs are associated with some serious diseases such as amyotrophic lateral sclerosis (Y. R. Li et al., 2013) or cancer (Anderson et al., 2015). Many studies also connect oxidative stress to osteoporosis (Kimball et al., 2021; Zhao et al., 2021).

1.1.1. Oxidative stress and osteoporosis

The imbalance between reactive oxygen species and the cellular defence against these free radicals is known as oxidative stress. Together with apoptotic mechanisms, sex-steroid deficiency and macroautophagy, oxidative stress has been implicated as the main risk factor in the development of osteoporosis (Hendrickx et al., 2015).

As described in chapter 3.1, bone is a highly dynamic tissue that requires the coordinated engagement of concerned bone cell types: osteoblasts, osteoclasts, and osteocytes. The bone

remodelling process depends on the precise communication between these cells and several molecules such as cytokines, hormones, and growth factors. Oxidative stress disrupts these homeostatic mechanisms leading to the imbalance between osteoblasts and osteoclasts activity. Reactive oxygen species (ROS) have been shown to induce apoptosis of osteoblasts and osteocytes resulting in increased osteoclasts differentiation followed by a decrease in bone mass (Figure 3; Almeida et al., 2007).

The molecular mechanism behind the abovementioned events is mainly the activation of RANKL-RANK signalling between osteoblasts and osteoclasts precursors (Huh et al., 2006). As already described, RANKL binding to RANK leads to osteoclasts differentiation and their activation. This results in osteoclasts' survival and increased bone resorption. Several studies have shown that antioxidants have an opposing effect by supporting osteoblasts differentiation (Domazetovic et al., 2017).

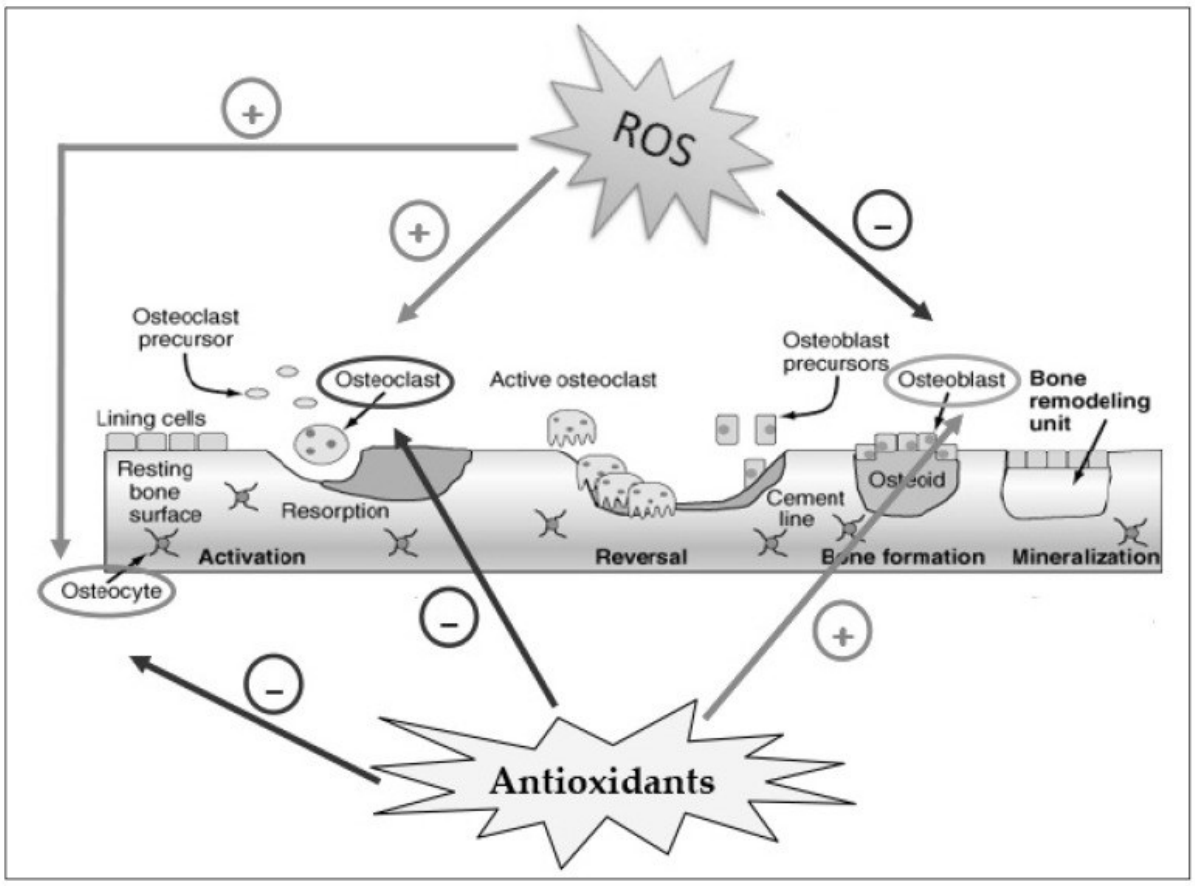

Figure 3*: Effect of ROS and antioxidants on the activity of osteoclasts, osteoblasts, and osteocytes in bone remodelling. ROS activate osteoclast differentiation and osteocyte apoptosis (+) and inhibit osteoblast activity (−) resulting in bone resorption; antioxidants activate*

osteoblast differentiation (+), while inhibiting osteoclast activity and osteocyte apoptosis (−) leading to bone formation, Adapted from Domazetovic et al., 2017

1.1.2. FUBP3 and stress granules

Stress granules and processing bodies are both cytosolic condensates that form by phase separation of proteins and RNAs. While SGs assemble around components of the translation machinery, the P-bodies consist mainly of proteins and mRNAs related to RNA decay (Stoecklin & Kedersha, 2013). High-throughput proximity mapping of stress granules and processing bodies performed by Youn et al. (2018) suggested that FUBP3 is a component of the SGs core proteome. Co-localization of two stress granule markers with FUBP3 is one of the goals of our study.

4. Aim of the work

We aim to elucidate the role of FUBP3 in pathways involved in the development of osteoporosis. To fulfil the stated objective, we will carry out an analysis of current knowledge about cell localization, expression and interactome. Alongside, we aim to create stress conditions for HeLa, A549, HOS, MG-63 and BM-MSC cells. The localization of FUBP3 in stressed and control cells will be investigated and detected via immunofluorescence microscopy. Localisation of stress granule markers PABPC1 and G3BP1 in the above-mentioned cells and co-localization with FUBP3 will be carried out.

We will test the following hypotheses:

1. FUBP3 interacts on a protein level with counterparts associated with osteoporosis and bone mineral density.

2. FUBP3 knockout in a human osteosarcoma cell line affects gene expression of certain osteoporotic markers and genes involved in the formation of bone tissue.

3. FUBP3 co-localizes with stress granule markers under stress conditions and is a constituent of stress granules.

5. Materials and methods

5.1. Chemicals and reagents

Chemicals:

- Ampicillin (Sigma Aldrich)
- Antibiotic/antimycotic (Biowest, 100x)
- Bovine serum albumin (BSA) (ThermoFisher Scientific)
- Dulbeccos‘ modified medium (DMEM) (Biowest)
- EvaGreen DNA-binding Dye (Solis BioDyne)
- Foetal bovine serum (FBS) (Biowest)
- Invitrogen ProLong Gold Antifade Mountant with DAPI (ThermoFisher Scientific)
- L-Glutamine (Biowest)
- PolyJet DNA InVitro Transfection (SignaGen Laboratories)
- RNaseZap (SigmaAldrich)
- Triton X-100 (SigmaAldrich)
- Trypsin (Biowest)
- 4% Paraformaldehyde (SigmaALdrich)
- 10x Phosphate buffer saline (PBS) (Lonza)

Antibodies:

- Anti-FUBP3 produced in mouse (sc-398466; Santa Cruz Biotechnology)
- Anti-PABPC1 produced in rabbit (HPA045423; Sigma Aldrich)
- Anti-G3BP1 produced in rabbit (HPA004052; Sigma Aldrich)
- Anti-mouse IgG Alexa Fluor 555 (A31570; Thermo Fisher Scientific)
- Anti-rabbit IgG Alexa Fluor 488 (A11008; Thermo Fisher Scientific)

Reagent Kits:

- High-Capacity cDNA Reverse Transcription Kit (Thermo Fisher Scientific)
- PeqGOLD Total RNA Kit (VWR)

Cells and cell lines:

- HeLa (ATCC)

- HOS (ATCC)
- A549 (ATCC)
- MG-63 wt (ATCC)
- MG-63 FUBP3 ko (Created at the Faculty of Pharmacy, University of Ljubljana, unpublished)
- BM-MSC (Lonza)

5.2. Bioinformatics analysis

To gather current knowledge about FUBP3, various databases were used. The Universal Protein Resource (UniProt) is a resource for protein sequence and annotation data which was used as a starting point for the whole inquiry.

5.2.1. Enzyme and pathway involvement

PathwayCommons, a tool collecting biological pathway and interaction data was used to scan FUBP3 involvement in biological pathways. The database provides a detailed representation of a variety of biological concepts including biochemical reactions, gene regulatory networks, genetic interactions, transport and catalysis events, and physical interactions involving proteins, DNA, RNA, and small molecules and complexes. The Kyoto Encyclopedia of Genes and Genomes (KEGG) pathway database was used as well.

5.2.2. Protein localisation

We used COMPARTMENTS - a weekly updated web resource that integrates data on protein subcellular localization from manually curated literature, high-throughput screens, automatic text mining, and sequence-based prediction methods. The Human Protein Atlas was also searched for localization information. The Human Protein Atlas is a Swedish-based program initiated in 2003 to map all the human proteins in cells, tissues, and organs using an integration of various omics technologies, including antibody-based imaging, mass spectrometry-based proteomics, transcriptomics, and systems biology.

5.2.3. Associated phenotypes and diseases

Organism-specific databases proposed by UniProt are DisGeNET, OpenTargets, and PharmGKB. All three were used to gain data about the association of FUBP3 expression and phenotype. DisGeNET is a publicly available collection of genes and variants associated with human diseases. DisGeNET data are homogeneously annotated with controlled

vocabularies and community-driven ontologies. The Open Targets Platform is a tool for access and visualization of potential drug targets associated with a disease. The Pharmacogenomics Knowledgebase is a resource providing data about how human genetic variation affects the response to medications. It collects and curates info about clinically actionable gene-drug associations and genotype-phenotype relationships.

5.2.4. Gene expression

Database for gene expression evolution Bgee allows comparison of gene expression patterns in multiple animal species. Also, data from the Human Protein Atlas was retrieved. To understand the regulation of expression, the Signaling Pathway Project (SPP) was researched. The SPP is a multi-omics knowledgebase allowing investigation of single gene's transcriptomics and cistromics.

5.2.5. Interactome

An interactome can be described as a network of macromolecular interactions and their interconnectivity. Understanding interactomes seems essential to understand the cell as a system and interactome mapping is the next step forward following genome sequencing. Interaction maps incorporate biophysical (direct contact or co-complex associations) and functional connections (involvement in a common process). Contemporary mapping strategies produce possible-interaction data that needs to be translated into functional relations. It is pivotal to integrate the functional and biophysical maps with co-expression and co-localization data to be able to present a fully understood interactome network (Luck et al., 2016).

In the following parts, interactions of FUBP3 with various biomolecules are gathered from different sources.

For acquiring data about FUBP3 protein-protein interactors, several databases were scanned. Information was gathered from UniProt, IntAct, DIP, BioGRID, MINT, STRING, and Proteomics DB. The protein interaction database and analysis system (IntAct) collects interactions derived from literature curation or direct user submissions. Database of Interacting Proteins (DIP) is a database that catalogues experimentally determined interactions between proteins. The Biological General Repository for Interaction Datasets (BioGRID) is a resource of manually curated protein and genetic interactions. The Molecular INTeraction database (MINT) focuses on experimentally verified protein-protein interactions. STRING (functional

protein association networks) was used to retrieve protein-protein interactions. STRING is a database of known and predicted protein-protein interactions. The interactions include direct (physical) and indirect (functional) associations. They stem from computational prediction, knowledge transfer between organisms, and interactions aggregated from other (primary) databases. Proteomics DB comprises collections of mass spectrometry-based proteomics data.

5.2.6. Protein interactors connection to osteoporosis/bone mineral density

The OpenTargets platform previously used to learn about FUBP3-associated phenotypes was used now to determine which of the interactors are associated with bone mineral density or osteoporosis. This process created a list of FUBP3 protein-protein interactors that might together be part of a pathway responsible for the pathological processes of OP. The interactors were then checked for GO Annotations connected to Wnt-signalling, osteoblast differentiation or proliferation, and ossification in bone maturation. Some of these hits were then chosen as genes of interest for qPCR expression analysis.

5.3. Cell culturing

5.3.1. Cell thawing

The cell lines are stored in liquid nitrogen below -135 °C. The cells are thawed, prior to the experiments. Cryovials containing frozen cells were taken out and heated to 37 °C for a minute. As the cells are frozen in toxic 10 % dimethyl sulfoxide, instant dilution with 10 % FBS DMEM is a critical step in maintaining viable cells. The cells in DMEM are then to be transferred to a culture dish and kept at 37 °C, 5 % CO_2 until the next day. To check growth progress, the cells are inspected under a microscope. The old DMEM replaced by fresh low-glucose DMEM with 10 % FBS, 1 % glutamine, and 1 % antibiotic/antimycotic.

5.3.2. Cell subculturing

Cell subculturing is done by transferring all or some cells to new growth media. To keep the cell lines healthy and viable, regular sub-culturing is crucial, as by letting the cells reach complete confluency, we are risking the cells changing their gene expression patterns. Also by subculturing, we can expand the number of cells we can work with. In aseptic conditions, old culturing media was aspirated and washed with 1x PBS. All cell lines we worked with are

adherent types of cells. To detach the cells, 2 ml of 0.25 % Trypsin solution was added and incubated at 37 °C for 4 minutes. Further trypsinization was prevented by addition of fresh low-glucose DMEM supplemented with 10 % FBS, and 1 % glutamine. The suspension of cells was then ready for seeding or transfer to a new dish.

5.3.3. Cell seeding

The cells were seeded in a 12-well plate on a glass coverslip in order to be able to take the adherent cells out later for staining. Cells were seeded at the density of $2x10^5$ cells/ml. First, the medium was aspirated from the dish. The cells were washed with 1x PBS and trypsinized using 2 ml of 0.25 % Trypsin solution. After 4 minutes of incubation at 37 °C, low-glucose DMEM was added to terminate trypsinization. After this step, the cells detached from the surface and are ready to be seeded.

5.4. Stress induction in HeLa, MG-63, A549, HOS and BM-MSC cells

The cells were seeded in a 12-well plate at $2x10^5$ cells/ml density and incubated at 37 °C and 5% CO_2 overnight. The next day, cells were heat treated at 44°C, 5% CO_2 atmosphere for 45 minutes. The control group was left at 37° C. Immediate fixation was done to avoid the cells recovering from stress induced by increased temperature. The cells were washed once with 1x PBS. Then fixed with 4 % PFA and incubated at 37 °C for 15 minutes. Later, the cells were washed with 1x PBS twice for 5 minutes and kept in 1x PBS at 4 °C until the next day for staining. The plate was sealed with parafilm.

5.5. Immunostaining of investigated proteins and fluorescence microscopy

5.5.1. Immunostaining of investigated proteins

The following protocol was employed for immunostaining of concerned proteins. The medium was aspirated from the wells and the cells were washed with 1x PBS. The next step was the permeabilization of cells. Hence, we added 300 µl of 3 % BSA and 0.2 % Tween in 1x PBS to each well and incubated for 5 minutes at RT. Afterwards, cells were washed with 1x PBS twice for 5 minutes. Next, 300 µl of 3 % BSA was added to each well and incubated for

20 minutes at RT. This step is done to avoid unspecific binding of antibodies to non-target structures. The cells were then washed twice with 1x PBS, each washing being 5 minutes. Finally, 200 µl of primary antibodies was added to each well and incubated for 2 hours at RT, followed by 1x PBS washing - twice for 5 minutes. At the end, 200 µl of secondary antibodies was added and incubated for 45 minutes in the dark. Again, the cells were washed twice with 1x PBS.

5.5.2. Immunostaining of FUBP3

To visualize FUBP3 in cells, the following antibodies were used: anti-FUBP3 produced in mice as pAb; donkey anti-mouse IgG conjugated with AF555 as sAb. The dilution of pAb was 1:200 and sAb 1:1000. All antibodies were diluted in 3 % BSA in 1x PBS. The emission maximum of AF555 is 568 nm and it emits orange light after exposure to 555 nm.

5.5.3. Optimization of PABPC1 and G3BP1 staining

Different dilutions of antibodies were used to stain PABPC1 as shown in Table 1. As the primary antibody, rabbit anti-PABPC1 was used. The secondary antibody was goat anti-rabbit IgG conjugated with AF488 emitting green light after exposure to 499 nm. All antibodies were diluted in 3 % BSA in 1x PBS. Following dilutions were chosen for final experiments: 1:200 for pAb and 1:500 for sAb.

Table 1: Dilutions of pAb and sAb for PABPC1 staining

anti-PABPC1	anti-rabbit IgG
1:100	1:1000
1:200	1:500
1:500	
1:1000	

The same method was used for G3BP1 staining. The following optimal concentrations of antibodies were employed in the experiments: 1: 400 for G3BP1 and 1:500 for anti-rabbit IgG-AF488.

5.5.4. Co-staining of FUBP3 with PABPC1 or G3BP1

The fixed cells were washed thrice with 1x PBS. Next, the cells were permeabilized with 500 µl of 0.1 % Triton in 1x PBS three times for 5 minutes. The cells were washed twice for 5 minutes with 1x PBS. For blocking of nonspecific binding, 4 % FBS in 1x PBS was used. The cells were incubated for 20 minutes at RT. After washing twice for 5 minutes with 1x PBS, 200 µl of primary antibodies in the desired dilution was added (see Table 2), the plate was sealed with parafilm and put at 4 °C for overnight incubation (20 hours). The next day, 1x PBS washing four times for 10 minutes was done. Afterwards, 300 µl of secondary antibodies in the desired dilution was added and incubated at RT for 90 minutes. The cells were washed twice and prepared for microscopy.

Table 2: Dilution ratios of primary and secondary antibodies used for co-staining.

	FUBP3	PABPC1	G3BP1
pAb	1:200	1:200	1:400
sAb	1:1000	1:500	1:500

5.5.5. Immunofluorescence microscopy

Following the staining, microscopy glasses were prepared. A drop of ProLong Gold Antifade Mountant with DAPI was used to stain the nuclei. The coverslips were carefully removed from wells using forceps and placed on the drop of mountant cell-face down. To get rid of bubbles, the coverslips were gently pressed down. To fix the coverslips to microscopy glass, transparent nail polish was used. The glasses were left overnight in the dark at 4 °C to dry. The next day, nail polish was used to seal the coverslips in order to avoid further drying of the mountant.

For microscopy, the EVOS® FL Cell Imaging System from Thermo Fisher Scientific was used. Images covering different fluorescent channels were generated from each coverslip and then they were merged. A magnification of 20x and 40x was used for the pictures.

5.6. qPCR expression analysis of target genes in MG-63 wt and FUBP3 ko cells

5.6.1. RNA isolation

For the purpose of gene expression analysis, RNA had to be isolated from the cells. We isolated RNA from FUBP3 knockout (ko) and wild-type (wt) MG-63 cells. Before isolation, the laminar chamber was treated with ethanol and UV light. Also, RNaseZap (Sigma) was used to prevent any ribonuclease contamination. For RNA isolation peqGOLD Total RNA Kit was used.

For sample preparation, the medium was aspirated and cells were washed with 1x PBS. Trypsinization was ended after 4 minutes with the addition of DMEM. The cells were transferred from the dish to a falcon tube and centrifuged at 300 rcf for 5 minutes, the medium was aspirated. Next, 1 ml of 1x PBS was added and the cells were transferred to an Eppendorf tube. Both tubes, with ko and wt cells, were centrifuged at 300 rcf for 5 minutes.

In the first step of RNA isolation, 1x PBS was aspirated and RNA Lysis Buffer T (400 µl) was added. The lysate was transferred into a DNA Removing Column placed in a Collection Tube. Columns inside the Tubes were centrifuged at 12 000 rcf for 1 minute at RT. Flow-through was transferred to a new tube. An equal volume (400 µl) of 70 % Ethanol was added to the lysate and the mix was vortexed. Next, all the liquid was transferred to a PerfectBind RNA Column in a Collection tube and centrifuged at 10 000 rcf for 1 minute. The flow-through liquid was discarded. The PerfectBind RNA Column was washed with 500 µl RNA Wash Buffer I and centrifuged for 1 minute at 10 000 rcf. Flow-through liquid was discarded. Later, 600 µl of RNA Wash Buffer II was added to PerfectBind RNA Column and centrifuged at 10 000 rcf for 1 minute. Washing with RNA Wash Buffer II was done twice. The next step is drying. The PerfectBind RNA Column containing RNA was centrifuged for 2 minutes at 10 000 rcf to dry completely. To elute RNA, the PerfectBind RNA Column was placed in a 1.5 ml microcentrifuge tube and 50 µl of sterile RNAse-free water was added. Everything was centrifuged at 5 000 rcf for 1 minute.

RNA concentration was measured using the NanoDrop Spectrophotometer. The concentration of RNA is determined by the absorbance of 260 nm light. The ratio of absorbance at 260 nm and 280 nm is calculated to indicate the purity of the sample.

Isolated RNA was stored at -80°C.

5.6.2. Reverse transcription to cDNA

RNA was diluted to the same concentration for all of the samples, to produce the same quantity of cDNA. High-Capacity cDNA Reverse Transcription Kit (ABS) was used for reverse transcription. A solution of RT Buffer, dNTPs, Random Primers, RNAse inhibitor, dH_2O and Multiscribe Reverse Transcriptase was prepared as instructed in Table 3. 20 µl of the mix was added to 20 µl of each sample.

Table 3: Composition of solution for reverse transcription. High Capacity Reverse transcription kit (ABS) was used for reverse transcription.

Reagent	Volume [µl]
dH_2O	6.4
10x RT Buffer	4
25x dNTPs	1.6
10x Random Primers	4
RNAse Inhibitor	2
Multiscribe Reverse Transcriptase 50	2

The transcription was carried out in a Thermal Cycler by Applied Biosystems. The following reaction conditions were employed: 25 °C for 10 minutes, 37 °C for 120 minutes, 85 °C for 5 minutes and in the end the chamber cools down to 4 °C until cDNA is taken out and stored at -20 °C.

5.6.3. qPCR analysis

The acquired cDNA was diluted to the desired concentration. A master mix for each investigated gene consisting of specific forward and reverse primers, dH_2O and EvaGreen Dye is prepared and 9 µl of the master mix (see Table 4) is pipetted to each well. Next, 6 µl of cDNA is pipetted. Water was used as negative control.

Table 4. Master mix for qPCR composition add cDNA

Reagent	1 well [µl]	8 wells [µl]	18 wells [µl]
dH_20	5.7	45.6	102.6
Primer Fw 20µM	0.150	1.2	2.7
Primer Rev 20µM	0.150	1.2	2.7
EvaGreen (Solis) 5x	3	24	54

The plate was sealed and centrifuged for 2 minutes at 1 900 rpm. Next, the plate was placed in Roche LightCycler LC480 with the following settings:

Program	**Temperature(°C)**	**Time**	**Number of cycles**
Starting denaturation	95	12 min	1
denaturation	95	15 s	45–55
annealing	60–65	20–30 s	
extension	72	20–30 s	

In the first experiment standard curve method was used to calculate the concentration of DNA in the samples. For that purpose, a set of 5 standards was prepared to draw a standard curve. In the subsequent experiments, absolute concentration was not determined and the Livak method was used instead. The Livak method provides relative quantification, which means it compares the target gene expression post-treatment to an untreated group. A housekeeping gene, whose expression is not affected by the treatment, is used to control any differences in starting cDNA quantities. For our purposes, RPLP0 was chosen.

Table 5: Forward and reverse primers used in qPCR of investigated genes and RPLP0 produced by Macrogen

RPLP0	Fw: TCTACAACCCTGAAGTGCTTGAT Rev: CAATCTGCAGACAGACACTGG
QKI	Fw: GTGTATTAGGTGCGGTGGCT Rev: ATAGGTTAGTTGCCGGTGGC
SYNCRIP	Fw: TCTGTTGTCCCGTACTTGCC Rev: AGCTGTAACACTTGGAGACACT
PUF60	Fw: AATGGAAACCTCCACAGGGC Rev: GGCGTACTTCTTGGCCTTCT
APP	Fw: TGGAGGTACCCACTGATGGT Rev: GCACCAGTTCTGGATGGTCA
TMEM64	Fw: GCCAGACTGACACCCATACC Rev: AGCACACTAGGCTCTTGACA
PTEN	Fw: CAGCAGCTTCTGCCATCTCT Rev: TGCTTTGAATCCAAAAACCTTACT
TNRC6A	Fw: GTGCACTTTACACACATGAGAGAAT Rev: TGCTGTGGAAGTGCCGTTAT
RUNX2	Fw: AGCAAGGTTCAACGATCTGAGAT Rev: TTTGTGAAGACGGTTATGGTCAA
COL1A1	Fw: GCCAAGACGAAGACATCCCA Rev: GTTTCCACACGTCTCGGTCA
OC	Fw: AAGAGACCCAGGCGCTACCT Rev: AACTCGTCACAGTCCGGATTG
FGF	Fw: CTCCGCCCGGCTACAAC Rev: TAAGATGCACGGGCTACGTC

hMPP7	Fw: TTATACCCGGCAGCAAAGAG Rev: TGAGGCTGAACATCCAACAA
C-MYC	Fw: TGAGGAGACACCGCCCAC Rev: CAACATCGATTTCTTCCTCATCTTC
TMEM64 (2)	Fw: GCCAGACTGACACCCATACC Rev: AGCACACTAGGCTCTTGACA

5.7. Statistical analysis

Our interactome analysis only aims to create an overview of FUBP3 interactions across all mentioned databases, not to evaluate the strength of the interaction evidence.

Secondly, we performed a pilot qPCR analysis for bone mineral density and/or osteoporosis associated targets who interact with FUBP3. As this was a pilot study, only one repeat has been done. Therefore, we could not statistically evaluate our results and they shall serve as signals for further studies.

Lastly concerning immunofluorescence microscopy – quantitative image analysis was not performed as the goal of our study is to prove the co-localization of targets, not to quantify their signals.

6.Results

6.1. Bioinformatics analysis

6.1.1. Enzyme and pathway involvement

To determine the involvement of FUBP3 in biological pathways, the UniProt online tool was used. Using the PathwayCommons tool recommended by the UniProt server and querying FUBP3 (Q96I24) 25 genes were revealed as interaction genes with FUBP3. Those are FBL, NDUFS4, PCBP2, SAV1, PUF60, RNF2, OBSL1, CAND1, OTUB1, SF1, BCOR, B9D2, TARDBP, COPS5, CUL7, PDHA1, GRB2, SEC16A, PYHIN1, RPA3, MOV10, RPA2, DICER1, RAB10 (Figure 4; Rodchenkov et al., 2020; accessed 06/02/2021).

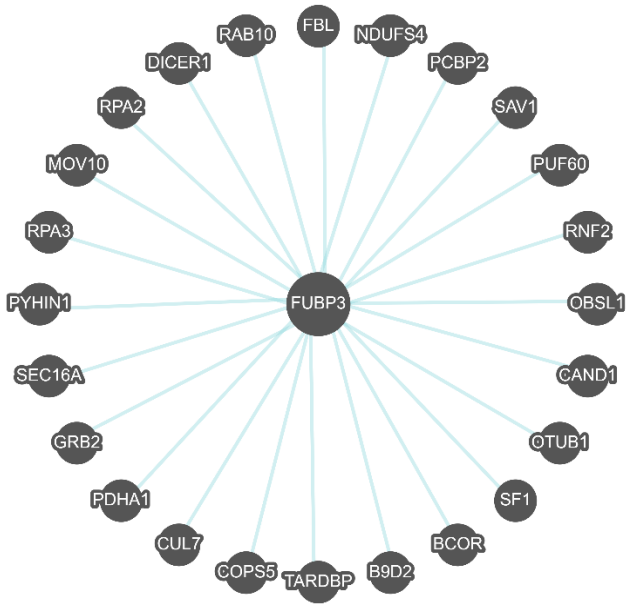

***Figure 4**: Interactions between FUBP3 and 25 genes; exported from Rodchenkov et al., 2020; blue lines mean binding of fubp3 to showed genes*

Using the OpenTargets Platform, we scanned the hits for connection to bone mineral density, bone fracture, and osteoporosis. Protein salvador homolog 1 (SAV1), B9 domain-containing protein 2 (B9D2), Helicase MOV-10 (MOV10), and Endoribonuclease Dicer (DICER1) show either genetic association or involvement in a pathway that is connected to bone development (Ochoa et al., 2021; accessed 21/02/2021).

We also searched the KEGG pathway database. KEGG is a database resource for understanding high-level functions and utilities of the biological system, such as the cell, the organism, and the ecosystem, from molecular-level information, especially large-scale molecular datasets generated by genome sequencing and other high-throughput experimental technologies. KEGG Pathway shows no hits for FUBP3 (Kanehisa et al., 2021; accessed 15/02/2021).

6.1.2. Cellular localization

Cellular localization of a protein is elementary knowledge that can provide insight into the protein's functions in a cell and on a higher level e.g. pathophysiology. In this case, functions of FUBP3 and its possible role in osteoporosis. According to a subcellular localization database COMPARTMENTS, the current knowledge about localization says FUBP3 is found in the nucleus, cytoplasm, and membrane (Binder et al., 2014; accessed 06/02/2021). Experimental results point to the nucleus and cytosol with weak - moderate evidence. Besides the above-mentioned, there are also predictions for cytoskeletal localization (Thul et al., 2017; accessed on 06/02/2021).

6.1.3. Associated phenotypes and diseases

DisGeNET (Piñero et al., 2020; accessed 07/02/2021) identifies 6 associations: Height, Body Height, Bone Density, Bone Mineral Density, Glomerular Filtration, and Liver Carcinoma. However, we believe "height" and "body height" are one anthropometric parameter, as well as "bone density" and "bone mineral density" are interchangeable terms. In summary that would give 4 associations for FUBP3.

OpenTarget (Ochoa et al., 2021; accessed 07/02/2021) identified 82 entries associated with FUBP3 altogether. With a cutoff set to 0.25 of the overall association score, only 12 remain. Besides various proportions of the body also BMD and bone fracture.

PharmGKB recognizes the FUBP3 gene, however, it shows no annotations (Whirl-Carrillo et al., 2012; accessed 07/02/2021).

6.1.4. Gene expression

Expression of the FUBP3 gene has been detected in several cells on mRNA and/or protein levels. According to the Bgee (data base for gene expression evolution), FUBP3 is expressed in 239 anatomical entities (Bastian et al., 2021; accessed 07/02/2021). To get additional

information, The Human Protein Atlas was used. FUBP3 is considered to have low tissue, cell type, immune cell type, and human brain regional specificity (Figure 5) (Uhlén et al., 2015; accessed 07/02/2021).

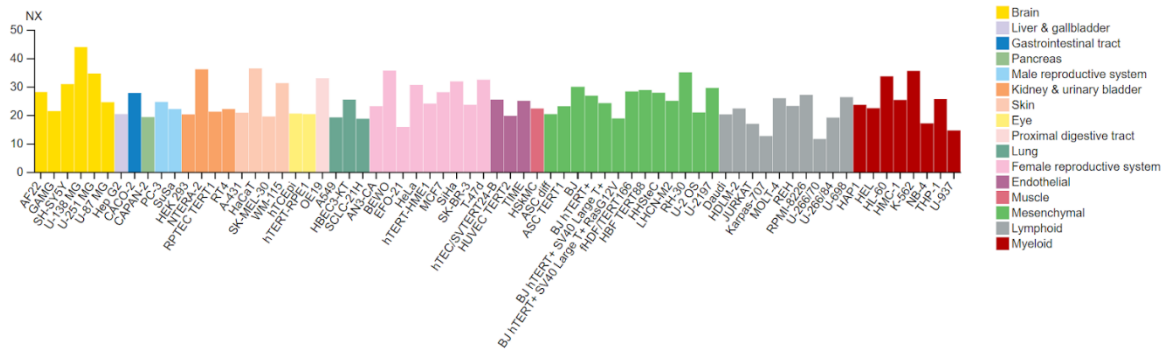

***Figure 5**: Expression of FUBP3 across cell lines and tissues; adapted from Uhlén et al., 2015*

6.1.4.1. Regulation of gene expression

To gain an overview of FUBP3 transcription regulation, we searched the Signaling Pathways Project. The query on the Signaling Pathways Project shows the FUBP3 gene's differential transcription under the influence of several factors.

More than 15 negative fold change of FUBP3 expression was found in experiments where human intestinal enteroids were treated with transforming growth factor β receptors1/2 inhibitor LY761 (-17.13 fold change) or TGFB1 (-23.84). The biggest positive fold change was found in an experiment where Human HLE B-3 lens epithelial cells were treated with dexamethasone (3.11 fold change). The complete results are shown below in Table 6 (Becnel et al., 2017; accessed on 19/02/2021)

Table 6. Differential expression of FUBP3 under the influence of small molecules or upon transfection; exported from Becnel et al., 2017

Tissue	Fold Change	P-value	Bioactive small molecule	Transfection
hepatocytes, 1° cells	2.677194034	0.00000717	NEFAZ	
epidermis, melanoma, Ma-Mel-15 cells	-2.010247947	0.045099802		JUN + MITF siRNAs
other, neuroglia, astrocytoma, U251 cells	-2.134163084	9.2E-09		TLX/NR2E1 siRNA
epithelium, MCF-7 cells	-2.019680832	0.005214554		RAF1.
epithelium, Snu-5 cells	-2.259523924	1E-10	PHA665	
small intestine, enteroids	-23.84116615	0.005010484	TGFB1	
cervix, epithelial, HeLa cells	-2.099318192	0		PHF8 siRNA
eye, lens, epithelium, HLE B-3 cells	3.112444261	0.010602402	DEX	
epithelium, MCF-7 cells	2.014124224	0.001356745	INS	
endometrium, epithelium, Ishikawa cells	2.112136874	0.000116967	BPA	
epithelium, PC3 cells	2.462319521	0.016849431		AR expression vector
epidermis, melanoma, Ma-Mel-15 cells	-2.182382738	0.027170109	TNF	
small intestine, enteroids	-17.13114629	0.008552968	LY761	
epithelium, MCF-7 cells	-2.453873431	0.0000415		ERBB2
hepatocytes, 1° cells	2.357191565	0.00000275	PTU	
CLL, unspecified, 1°	2.299772121	0.023061359	CDKI73,FLUDARA	
fibroblasts, keloid	-2.049241667	0.000000467	CORT	
myeloid lineage, promyelocytes, APL, HL-60 c	-2.112507161	0.006073641	ATRA	
epithelium, MCF-7 cells	-2.017701574	0.005171252		MAP2K1

6.1.5. Interactome

In the following part, FUBP3 interaction hits will be sorted by databases.

UniProt

In UniProt (Consortium, 2021) database search, 2 binary interactions with FUBP3 were identified: “QKI_HUMAN” (Protein Quaking) and “RBPS2_HUMAN” (RNA-binding protein with multiple splicing 2).

IntAct

The protein interaction database and analysis system (IntAct) shows 83 binary interactions for FUBP3 (Orchard et al., 2014; accessed 08/02/2021). After filtering out spoke expansions (spoke expansion links the bait molecule to all prey molecules), 7 interacting proteins remain. Besides previously mentioned QKI and RBPS2, interactors PUF60 (Poly(U)-binding-splicing factor), GRB2 (Growth factor receptor-bound protein 2), E7 (Protein E7 – HPV type 16 protein), ATXN1 (Ataxin-1), SF1 (Splicing factor 1) are reported.

DIP

Database of Interacting Proteins (DIP), a database that catalogues experimentally determined interactions between proteins, shows only 1 interactor for FUBP3 and that is PUF60 (Salwinski et al., 2004; accessed 08/02/2021).

BioGRID

The Biological General Repository for Interaction Datasets (BioGRID), a resource that houses manually curated protein and genetic interactions from multiple species, accessed on 08/02/2021, identifies 276 interactions with 227 unique interactors, of which 226 are physical interactors and one genetic (TP53 – tumour protein p53). Filtered for H. sapiens, 223 interactors remain (Oughtred et al., 2021). Listed interactors are identified by both low and high-throughput methods. The interactors are gathered in supplementary materials chapter 10.1.

MINT

The Molecular INTeraction database (MINT), which focuses on experimentally verified protein-protein interactions, identifies 15 interactions (Licata et al., 2012; accessed 09/02/2021). Only 10 are Homo sapiens proteins: Fragile X Messenger Ribonucleoprotein 1, Tudor Domain Containing Protein 3 and transcriptional regulators – forkhead box proteins FOXA3, FOXB1, FOXE1, FOXF1, FOXL2, FOXP3, FOXQ1, and FOXS1.

STRING

Furthermore, STRING (functional protein association networks) was used. STRING is a database of known and predicted protein-protein interactions. The interactions include direct (physical) and indirect (functional) associations. They stem from computational prediction, knowledge transfer between organisms, and interactions aggregated from other (primary) databases. STRING predicts 10 functional partners for FUBP3 based on coexpression, experiments, text mining, and homology. These partners are PUF60, FUBP1, NQO1, PCBP2, QKI, ARF4, HNRNPF, KHDRBS3, DAZAP1, and KHDRBS2.

However, STRING identifies up to 54 interactors with a minimum required interaction score set to 0.400 with sources in text mining, experiments, databases, a neighbourhood of genes, gene fusion, co-occurrence, and co-expression (Szklarczyk et al., 2019; accessed 09/02/2021).

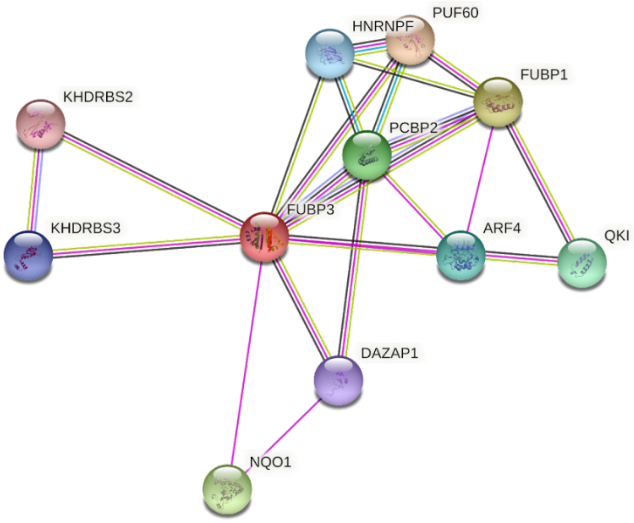

***Figure 6**: FUBP3 interactors by STRING database, adapted from Szklarczyk et al., 2019*

ProteomicsDB

Inquiry about FUBP3 on Proteomics DB suggests the following interaction network for FUBP3 – Table 7 (Samaras et al., 2020; accessed 09/02/2021)

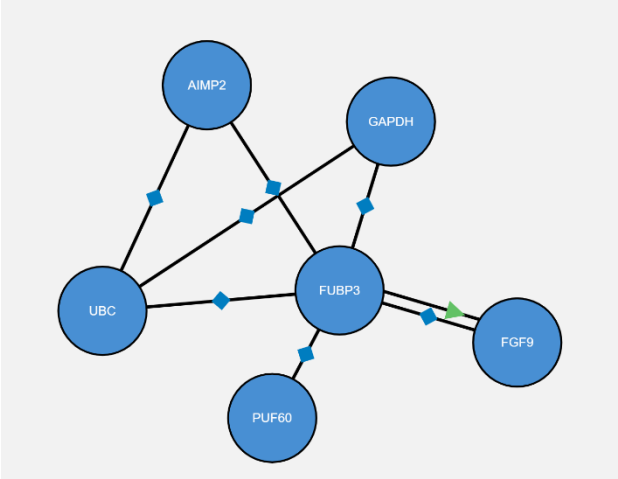

***Figure 7**: FUBP3 interaction network by Proteomics DB; Nodes represent protein interactions based on experimental data from STRING and KEGG. Besides binding (lines with blue square) to AIMP2, GAPDH, UBC, PUF60, and FGF9, the network also shows activation of FGF9 by FUBP3 (line with green arrow). Adapted from Samaras et al., 2020*

6.1.6. FUBP3's PPI association to BMD or OP

Again, the OpenTargets platform was used to determine which of the interactors are associated with bone mineral density or osteoporosis. Out of 326 human proteins interacting with FUBP3, 75 are associated with either bone mineral density (BMD), osteoporosis (OP), or both.

Associations are mostly genetic, some are based on text mining. The results are gathered in supplementary materials chapter 10.2.

The 10 top-scoring protein interactors associated with BMD alone are CPED1 (Cadherin-like and PC-esterase domain-containing protein 1), KLHL42 (Kelch-like protein 42), ZBTB10 (Zinc finger and BTB domain-containing protein 10), OTUD4 (OTU domain-containing protein 4), SMARCAD1 (SWI/SNF-related matrix-associated actin-dependent regulator of chromatin subfamily A containing DEAD/H box 1), XRN1 (5'-3' exoribonuclease 1), LIN7C (Protein lin-7 homolog C), MOV10 (Helicase MOV-10), IGF2BP2 (Insulin-like growth factor 2 mRNA-binding protein 2), and ITGA4 (Integrin alpha-4). Their association scores are ranging from 1.00 to 0.68 on a 1-0 scale. The basis of their connection to BMD is genetic.

The 12 top-scoring protein interactors associated with OP alone are CNOT3 (CCR4-NOT transcription complex subunit 3), METTL3 (N6-adenosine-methyltransferase catalytic subunit), TMEM64 (Transmembrane protein 64), VCAM1 (Vascular cell adhesion protein 1), PUM1 (Pumilio homolog 1), FOXA1 (Hepatocyte nuclear factor 3-alpha), NR2C2 (nuclear receptor subfamily 2 group C member 2), HDAC2 (histone deacetylase 2), ALG13 (ALG13 UDP-N-acetylglucosaminyltransferase subunit), UPF1 (UPF1 RNA helicase and ATPase), TP53 (Tumor protein p53), and KHDRBS1 (KH domain-containing, RNA-binding, signal transduction-associated protein 1). Their association scores are ranging from 0.27 to 0.03 on a 1-0 scale. The base of their connection to OP is text mining results, except for CNOT3 which has been shown to determine osteoporosis-like phenotype in Cnot3 deficient mice.

There are 9 protein interactors associated with both OP and BMD. Those are DICER1 (Endoribonuclease Dicer), QKI (Protein quaking), SYNCRIP (Heterogeneous nuclear ribonucleoprotein Q), FN1 (Fibronectin), PABPC4 (Polyadenylate-binding protein 4), TMEM57 (Macoilin), PTEN (Phosphatidylinositol 3,4,5-trisphosphate 3-phosphatase and dual-specificity protein phosphatase PTEN), CDK9 (Cyclin-dependent kinase 9), RHOA (Transforming protein RhoA).

6.1.7. Targets selected for in vitro expression analysis

Based on our bioinformatic analyses and relevance to bone metabolism the following targets were used for gene expression analysis in MG-63 FUBP3 knockout cell line:

Transmembrane protein 64 (TMEM64)

Transmembrane protein 64 has been selected as one of the targets for further investigation. TMEM64 was identified by STRING as a possible FUBP3 interactor with an overall confidence score of 0,599. Co-expression of orthologs has been previously observed in Mus musculus. Moreover, TMEM64 and FUBP3 are both possible targets of miRNA-223 in certain cell lines (Allantaz et al., 2012). TMEM64 has been reported to be an important regulator of osteoclast function by controlling Ca2+ oscillation in RANKL-mediated osteoclastogenesis (H. Kim et al., 2013). Knockout of the TMEM64 gene in mice showed increased osteoblast differentiation while the differentiation of adipocytes lowered. Overexpression inhibits osteogenesis and supports adipogenesis. Finally, TMEM64 is involved in the decision of mesenchymal cell fate by modulating Wnt/β-catenin signalling (Jeong et al., 2015). Reduced levels of TMEM64 mRNA were reported in osteoporotic patients' peripheral blood, making TMEM64 a promising marker for osteoporosis (Dera et al., 2019).

Amyloid-beta precursor protein (APP)

Another interactor chosen for further investigation is the Amyloid-beta precursor protein. APP has been recognized by the BioGRID database as an interactor based on a study done by Oláh and colleagues (2011) Amyloid precursor protein has been detected in bone of patients suffering from osteoporosis (Roos, 2014). Elevated mRNA and protein levels of APP have been recognized in human bone tissue as well as in osteoporotic rat model. Moreover, APP levels negatively correlate with BMD (S. Li et al., 2014). It was also demonstrated by Xia and colleagues (2013) that APP suppresses osteoblast differentiation and promotes osteoclast formation. The possibility of APP playing an important role in the pathophysiology of osteoporosis was also suggested by T. Wang and colleagues (2013).

Trinucleotide repeat-containing gene 6B protein (TNRC6B)

Trinucleotide repeat-containing gene 6B protein (TNRC6B) was reported by the BioGRID database as a FUBP3 interactor based on a dataset provided by Youn et al. (2018) TNRC6B is recognized as a genetic association for osteoporosis by OpenTargets Platform based on data from "Systematic comparison of phenome-wide association study of electronic medical record data and genome-wide association study data" (Denny et al., 2013). TNRC6B is involved in the Ca2+ pathway, a β-catenin-independent Wnt pathway (Jassal et al., 2020).

Helicase MOV-10

Helicase MOV-10 was identified as a FUBP3 interactor by PathwayCommons based on a paper by Hubel et al. (2019) as well as by BioGRID that adds Youn et al. (2018) to evidence supporting FUBP3 and MOV10 interaction. The genetic link between MOV10 and bone mineral density is supported by two genome-wide association studies performed by Kemp et al. (2017) and by Morris et al. (2018). Additionally, MOV10 is involved in the Wnt signalling pathway and calcium modulating pathway (Consortium, 2021).

Heterogeneous nuclear ribonucleoprotein Q (SYNCRIP)

Synaptotagmin Binding Cytoplasmic RNA Interacting Protein also known as Heterogeneous nuclear ribonucleoprotein Q was identified by BioGRID based on a dataset provided by Youn et al. (2018). The association of SYNCRIP with bone density is supported by 2 studies carried out by Kichaev et al. (2018) and Morris et al. (2018). SYNCRIP may be associated with the osteoporotic processes in the male population, it was found to be downregulated in patients. Furthermore, together with genes encoding haemoglobin subunits α1 and β, it might be involved in the pathophysiology of osteoporosis (Fei et al. 2020). Additionally, SYNCRIP is involved in the regulation of the Bone Morphogenic Protein pathway (Halstead et al., 2014). Based on data provided by Foster et al. (2005), SYNCRIP is also annotated in UniProt with osteoblast differentiation.

Fibroblast growth factor 9 (FGF9)

Interaction between FUBP3 and FGF9 was reported by Proteomics DB. This interaction is supported by evidence provided by Gau et al. (2011), who claim not only do FUBP3 and FGF9 interact but also that FUBP3 positively regulates the translation of FGF9. FGF9 itself plays an important role in bone development. It is suggested that FGF9 negatively regulates BMD, by inhibition of bone neoformation, while promoting osteoclastogenesis. Additionally, FGF9 can be considered a prospective therapeutical bone disease target (Tang et al., 2021). According to Watson & Adams (2018), administration of exogenous FGF9 supports bone repair after fracture, likely via mechanisms involved in the neovascularization of bone tissue. The genetic association between bone density and FGF9 is supported by two GWASs carried out by Morris et al. (2018) and S. K. Kim (2018).

Trinucleotide repeat-containing gene 6A protein (TNRC6A)

Trinucleotide repeat-containing gene 6A protein (TNRC6A), similarly to TNRC6B, was reported by the BioGRID database as a FUBP3 interactor based on a dataset provided by Youn et al. (2018). The genetic association between TNRC6A and bone mineral density is supported by studies by Morris et al. (2018) and Kichaev et al. (2018). Corresponding with the rest of GW182 (TNRC6 proteins), TNRC6A is also annotated with "Wnt signalling pathway, calcium modulating pathway" (Consortium, 2021) - meaning it is involved in the β-catenin-independent WNT Ca2+ pathway. The possible role of GW182 proteins in osteoporosis has not yet been explored.

Phosphatidylinositol 3,4,5-trisphosphate 3-phosphatase and dual-specificity protein phosphatase PTEN (PTEN)

BioGRID identifies PTEN as a FUBP3 interactor based on a dataset provided by Shen et al. (2019). The association of PTEN and bone mineral density is supported by 2 GWASs. (Kemp et al., 2017; Morris et al., 2018). Humtsoe et al. (2010) present evidence for PTEN to be involved in the canonical Wnt signalling pathway. A study by Sun et al. (2019) suggests that PTEN downregulation positively affects osteoblastogenesis. Y. Han et al. (2019) argue that the regulation of upstream molecules acting via PTEN could be promising therapeutic targets for osteoporosis. C. G. Wang et al. (2020) support this thesis and claim the expression of PTEN to "inhibit osteoclast differentiation and attenuate osteoporosis by suppressing the PI3K/AKT/NF-κB signalling pathway".

Transforming protein RhoA (RHOA)

Transforming protein Rhoa is identified in BioGRID as a FUBP3 interactor on account of evidence provided by Hein et al. (2015). OpenTargetsPlatform shows RHOA to be associated with both bone mineral density and osteoporosis. RHOA is functionally annotated with "regulation of osteoblast proliferation" and "ossification involved in bone maturation" which both point towards the possible importance of RHOA in bone tissue development (Consortium, 2021). According to Chellaiah et al. (2000), RHOA plays an essential role in osteoblast differentiation and bone resorption. Zeng et al. (2016) claim that RHOA is differentially expressed in osteoporotic patients, moreover, RHOA plays an important role in multiple pathways related to osteoporosis. Specifically, regulation of actin cytoskeleton, leukocyte transendothelial migration and Wnt signalling pathway. Altogether, differentially expressed RHOA is an important osteoporosis risk marker.

Additionally, Osteocalcin, COL1A1, and Runx have been chosen for qPCR analysis. Their role in bone biology is explained in the theoretical part of this thesis.

6.2. Subcellular localization of investigated proteins

6.2.1. Subcellular localization of FUBP3 in HOS, HeLa, A549, BM-MSC, and MG-63

An optimized method for FUBP3 staining in HeLa cells has been previously developed by J. Kunrt (2020) His protocol was used as a starting point for staining in other cell lines. FUBP3 staining could be observed in Hela, moreover, we show that the protocol is suitable and transferrable to HOS, A549, BM-MSC, and MG-63 cell lines (Figure 8).

As predicted in chapter 6.1.2, FUBP3 localizes in the cytoplasm. Weak signals can also be seen in nuclei or above/below as the cell is a 3D structure.

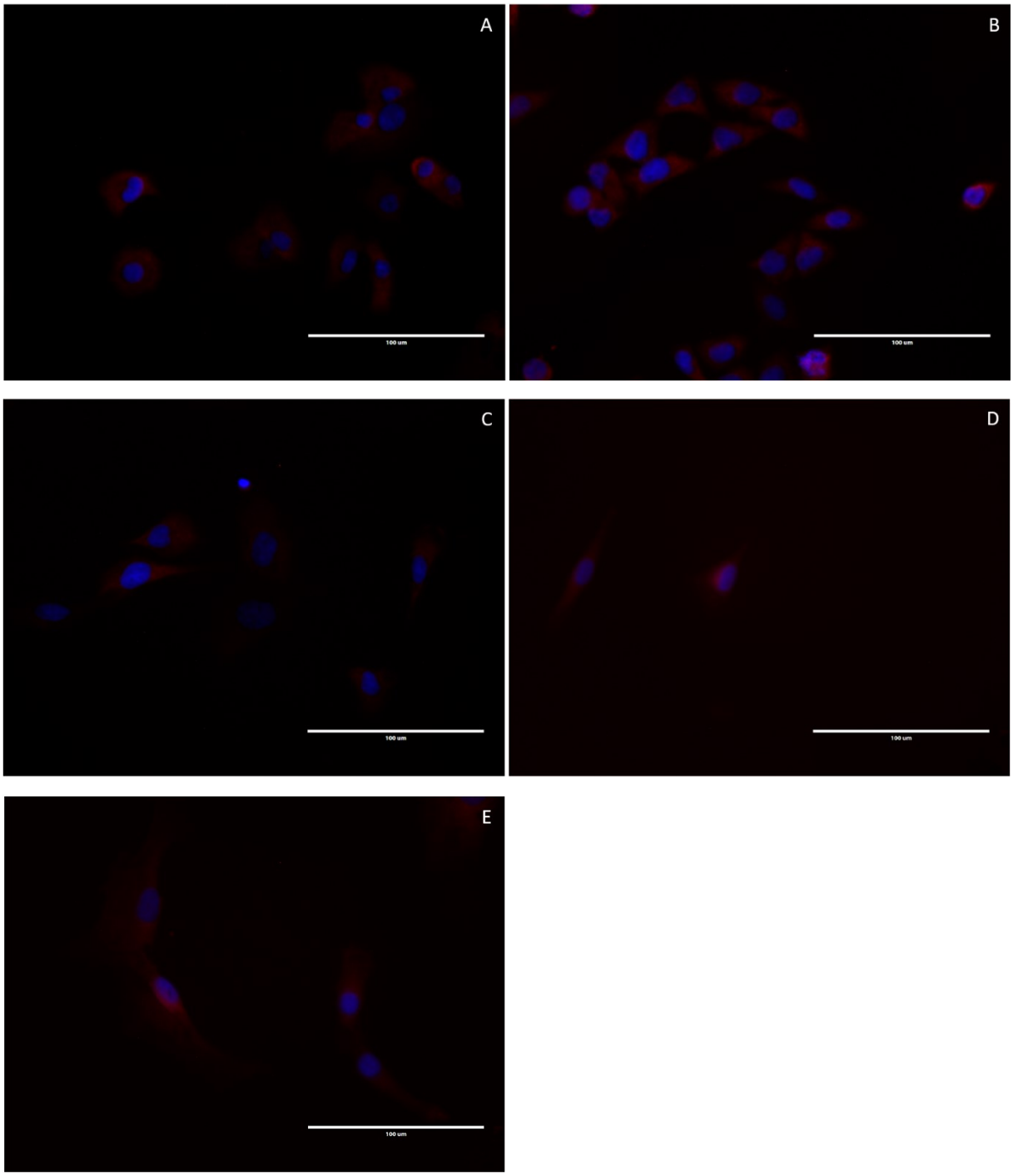

Figure 8*: anti-FUBP3 (red) and DAPI (blue) stained A549, HeLa, HOS, MG-63, and BM-MSC;* ***A****: A549;* ***B****: HeLa;* ***C****: HOS;* ***D****: MG-63;* ***E****: BM-MSC; Scale bar 100µm*

6.2.2. The localization of FUBP3 in heat-stressed HOS, HeLa, A549, BM-MSC, and MG-63

To test, whether FUBP3 cellular localization changes under stress conditions, the cells were exposed to heat as described in chapter 5.4. Upon introduction of stress, FUBP3 visibly forms clusters. (Figure 9)

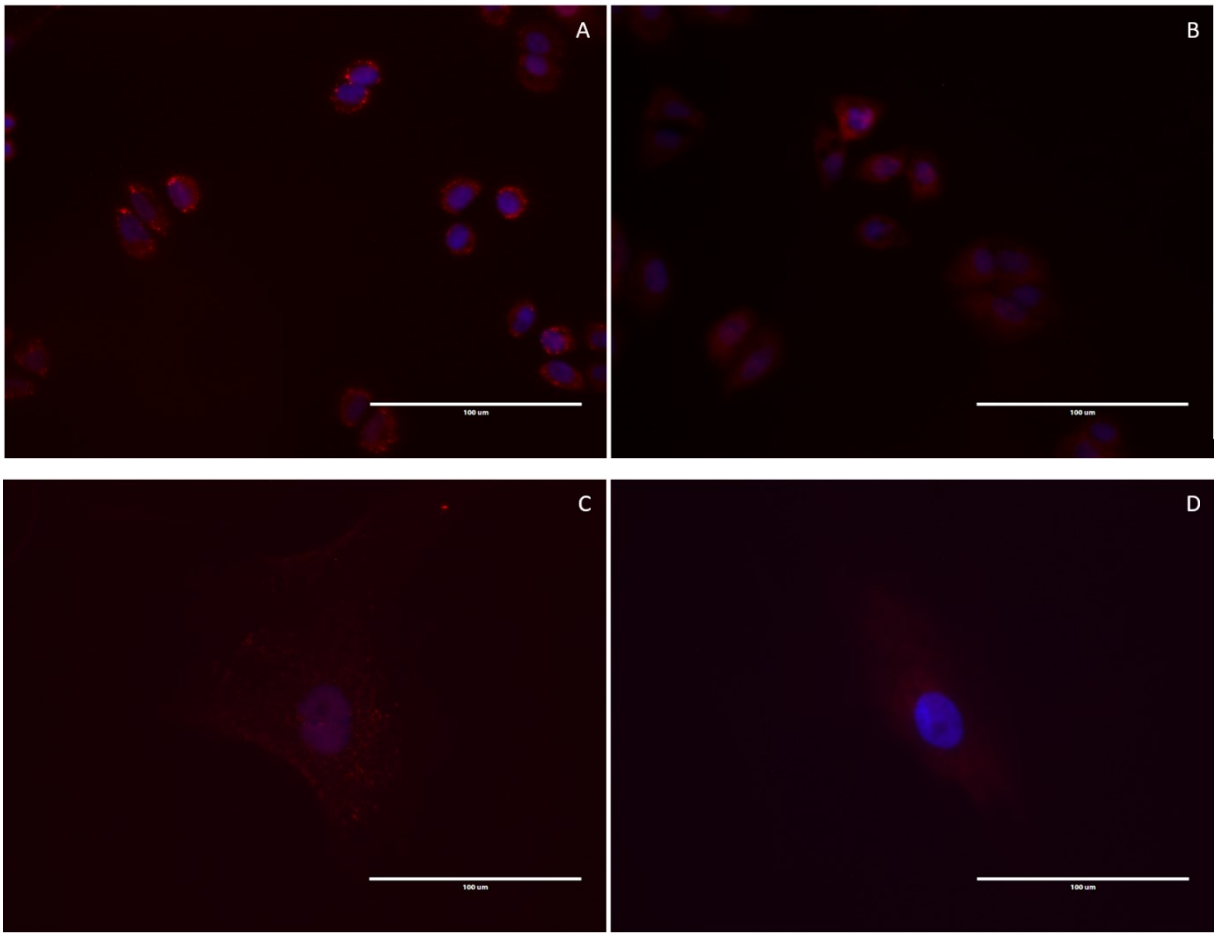

- the figure continues on the next page -

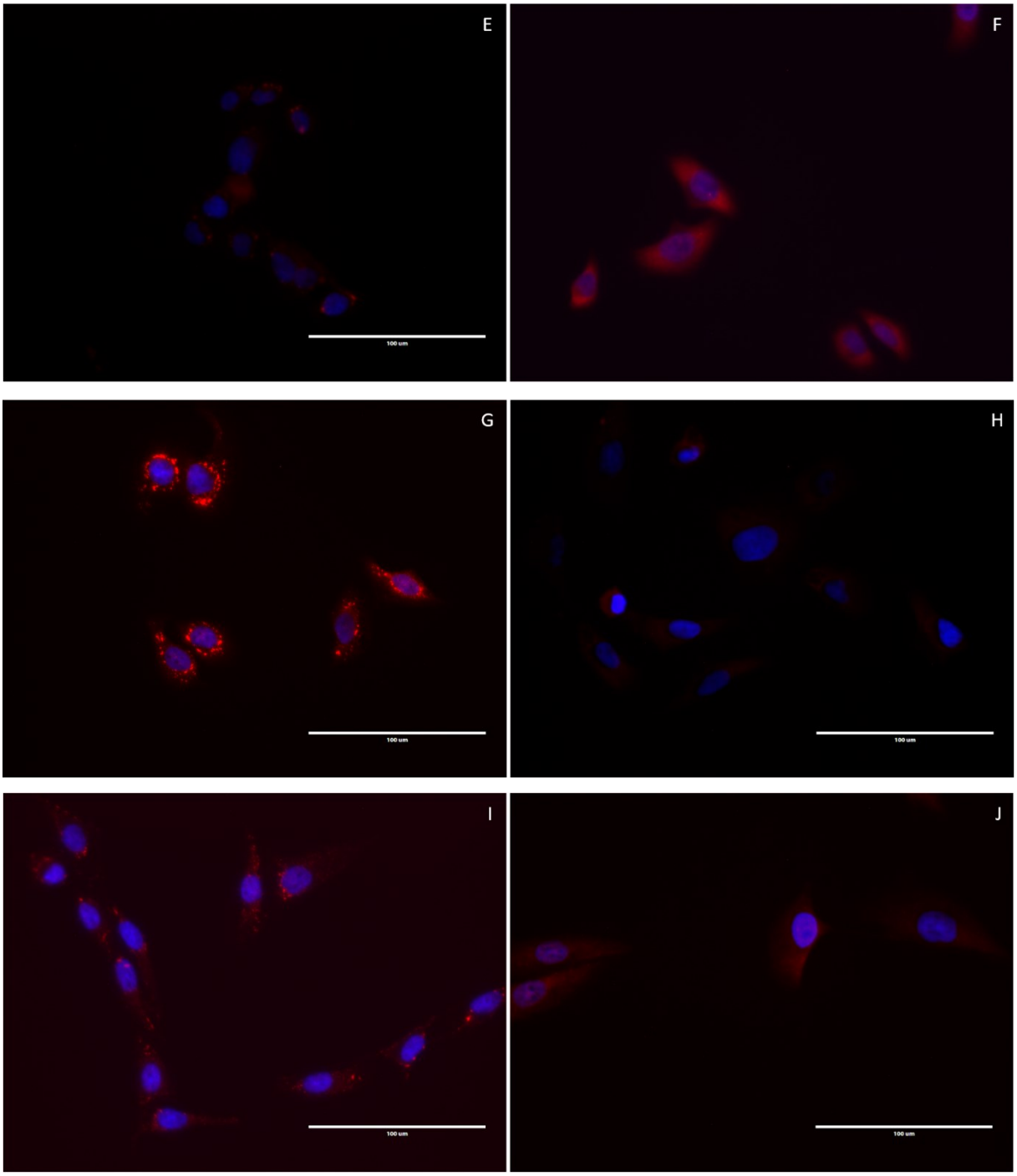

***Figure 9**: Localization of FUBP3 under stress conditions; left column represents images with treated cells, where clusters formed, and right column is the control group; red stained FUBP3, blue stained nuclei; **AB**: A549; **CD**: BM-MSC; **EF**: HeLa; **GH**: HOS; **IJ**: MG-63; Scale bar 100µm*

6.2.3. Co-localization of FUBP3 and stress granule markers PABPC1 and G3BP1

To examine whether FUBP3 co-localizes with the stress granules marker, the cells were stained for PABPC1 and G3BP1.

In the heat-treated A549 (Figure 10), HeLa (Figure 11), HOS (Figure 12) and MG-63 cells (Figure 13), significant formation of stress granules was observed as documented by an increase of PABPC1 marker (green). These granules are precisely overlapping with the granules of FUBP3 (red). In control samples, there are no visible granules of PABPC1 nor FUBP3. In the microscopy pictures, we observe blue-stained nuclei. The first two pictures **A - B** are untreated control. Pictures **C – D** show heat-treated cells, where distinct clusters of both PABPC1 and FUBP3 formed. In the last row, all DAPI, GFP and RFP channels are merged to show how PABPC1 co-localizes with FUBP3. Picture **E** are control cells and **F** are the stressed cells.

Detection of the other stress granules marker, G3BP1 protein, in the heat-treated A549 (Figure 14), BM-MSC (Figure 15), HeLa (Figure 16), HOS (Figure 17), and MG-63 (figure 18) was performed with similar results. For easier orientation, the figures are organized in the same manner as above. To repeat: the second stress granule marker G3BP1 is visualized in green, and FUBP3 is red. DAPI-stained nuclei are in blue colour. The first two pictures **A - B** are untreated control. Pictures **C – D** show heat-treated cells, where we observe granulation of both G3BP1 and FUBP3. In the last row, all DAPI, GFP and RFP channels are merged to show how G3BP1 co-localizes with FUBP3. Picture **E** are control cells and **F** are the stressed cells. There is no visible granulation of stained proteins in the control group.

Altogether, FUBP3 co-localized with both stress granule markers.

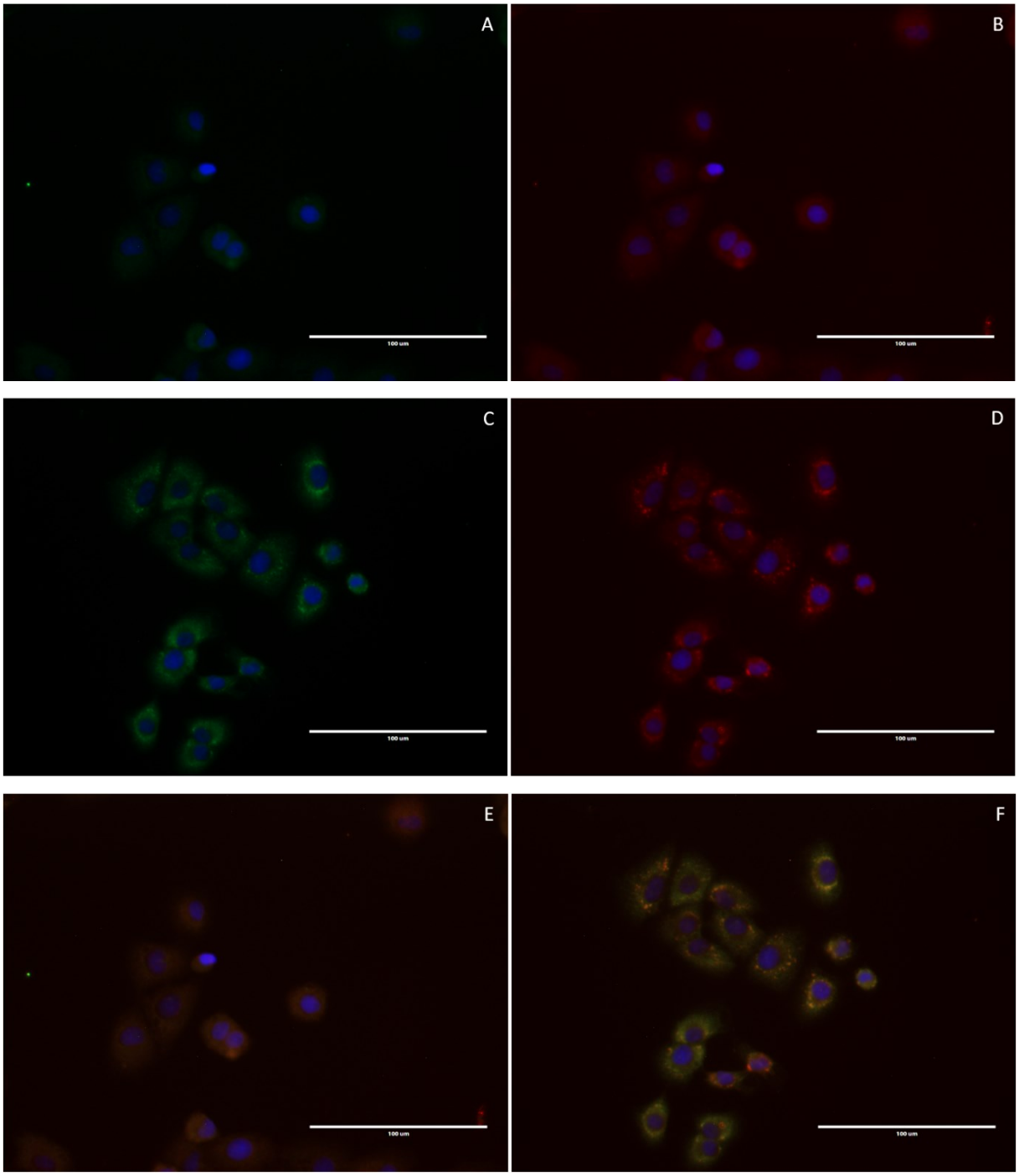

***Figure 10**: Localization of FUBP3 (red) and PABPC1 (green) in A549 cells*

AB: control; CD: stress group; E and F merged channels for control (E) and treatment (F)

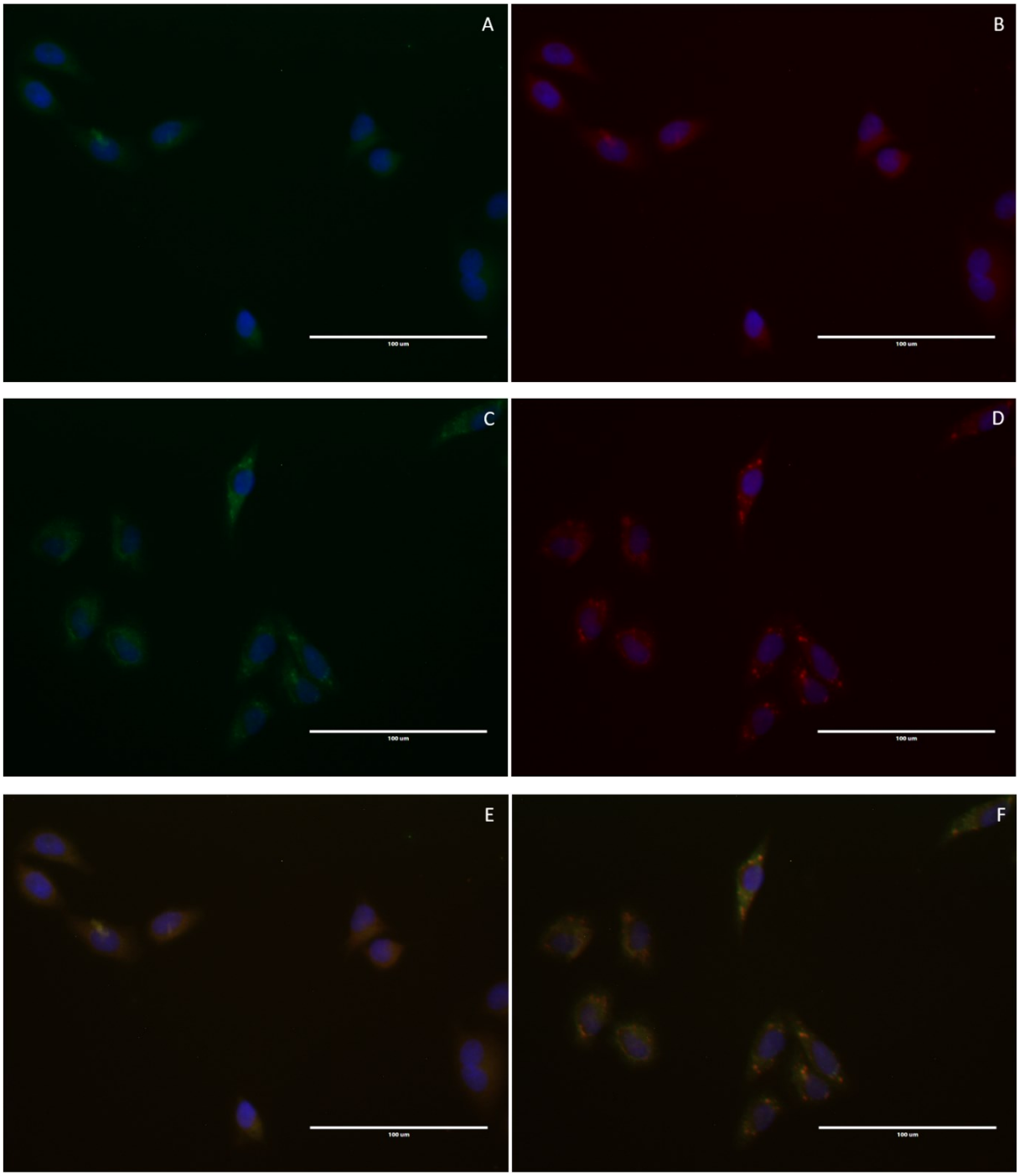

***Figure 11**: Localization of FUBP3 (red) and PABPC1 (green) in HeLa cells*

AB: control; CD: stress group; E and F merged channels for control (E) and treatment (F)

Scale bar 100 µm.

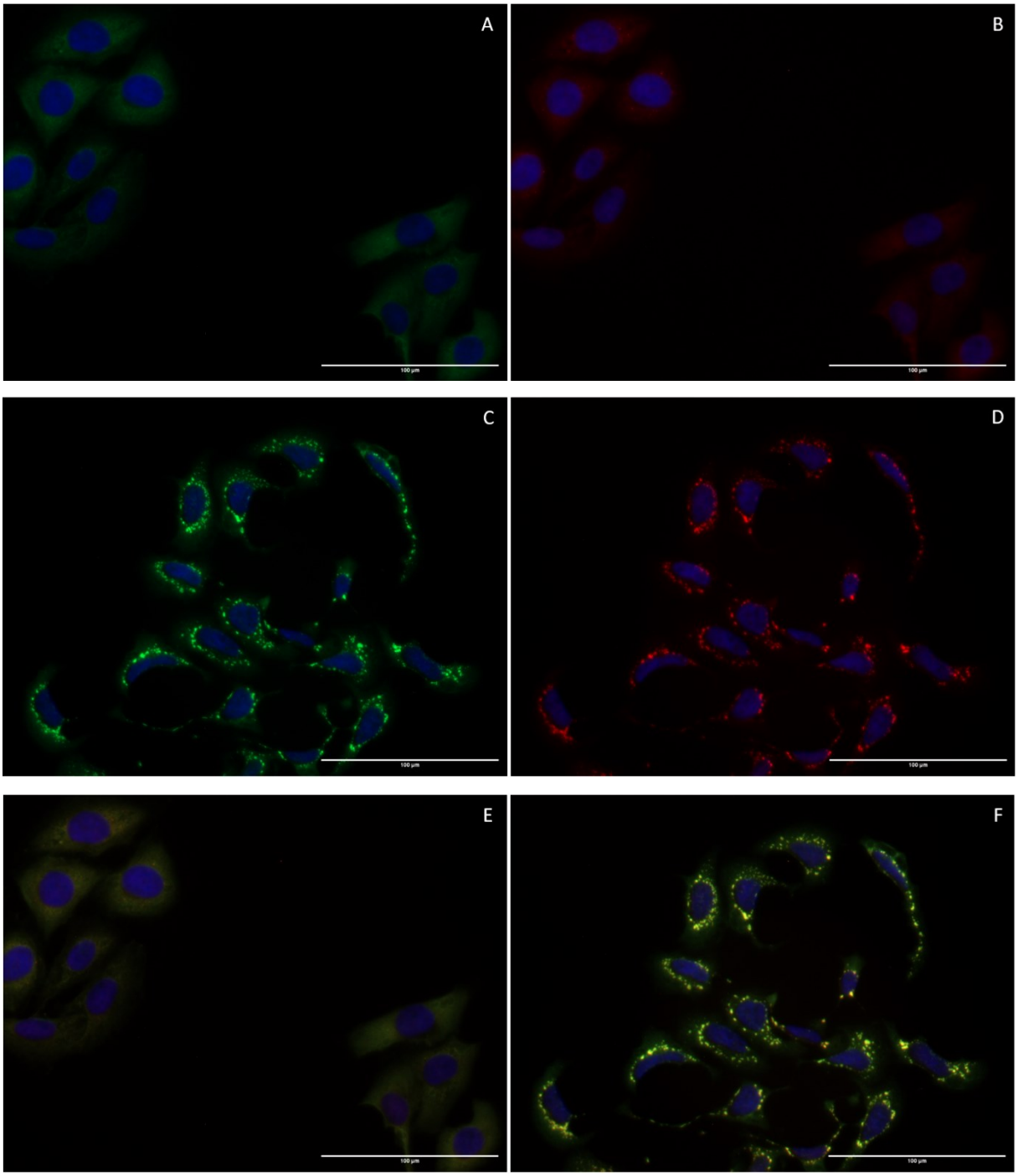

***Figure 12**: Localization of FUBP3 (red) and PABPC1 (green) in HOS cells*

AB: control; CD: stress group; E and F merged channels for control (E) and treatment (F)

Scale bar 100 µm.

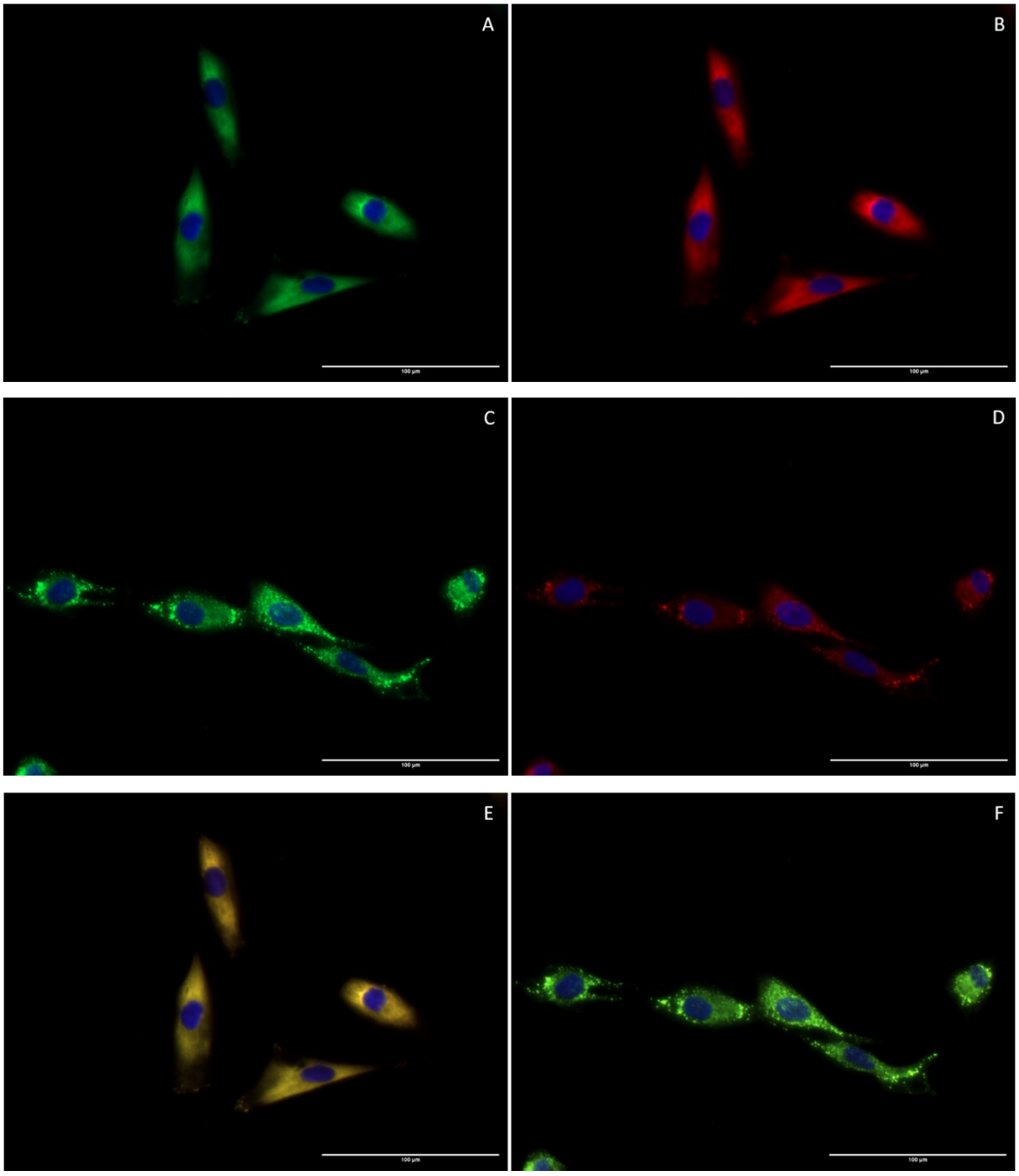

***Figure 13**: Localization of FUBP3 (red) and PABPC1 (green) in MG-63 cells*

AB: control; CD: stress group; E and F merged channels for control (E) and treatment (F)

Scale bar 100 µm

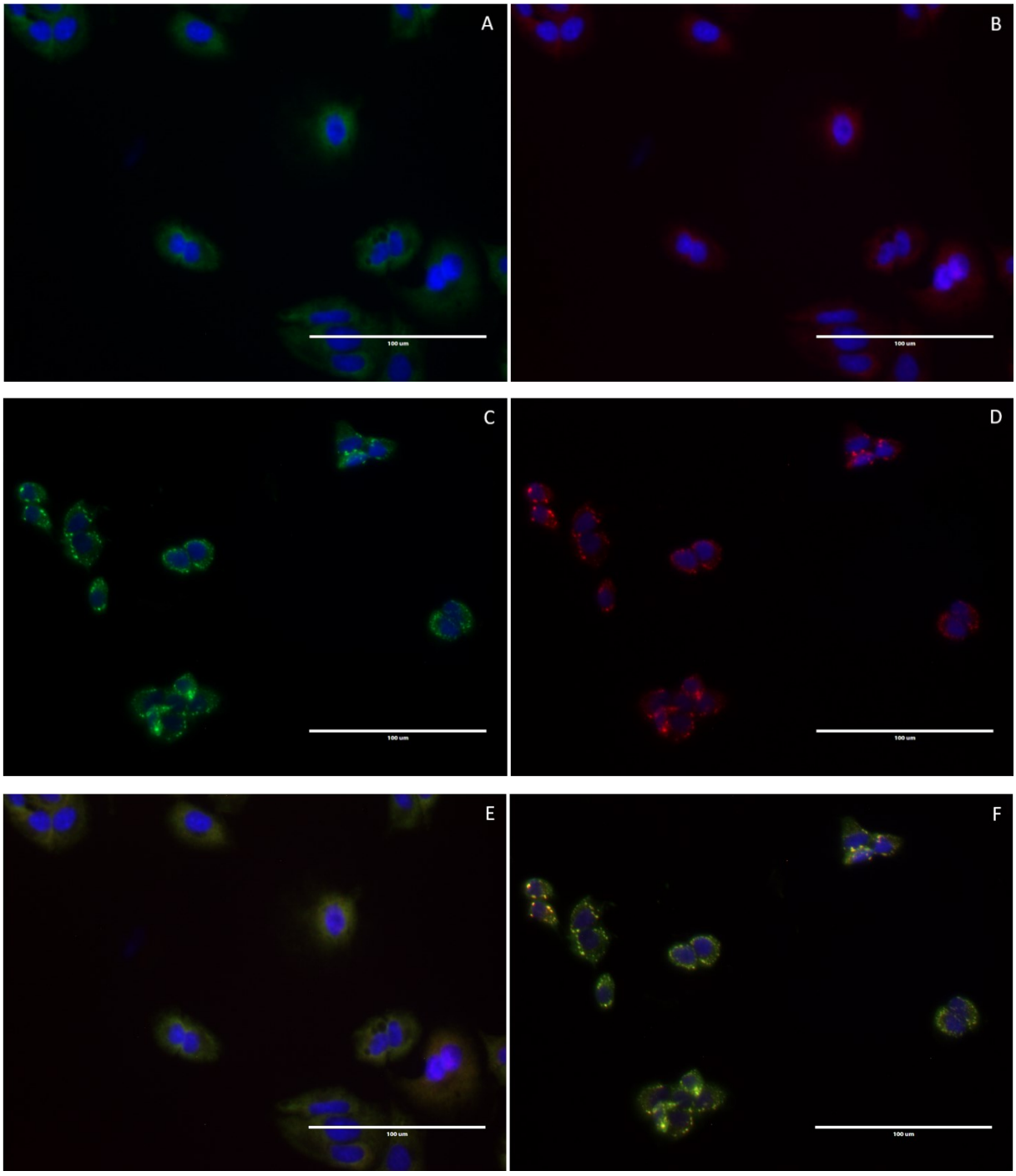

***Figure 14**: Localization of FUBP3 (red) and G3BP1 (green) in A549 cells*
AB: control; CD: stress group; E and F merged channels for control (E) and treatment (F)
Scale bar 100 µm.

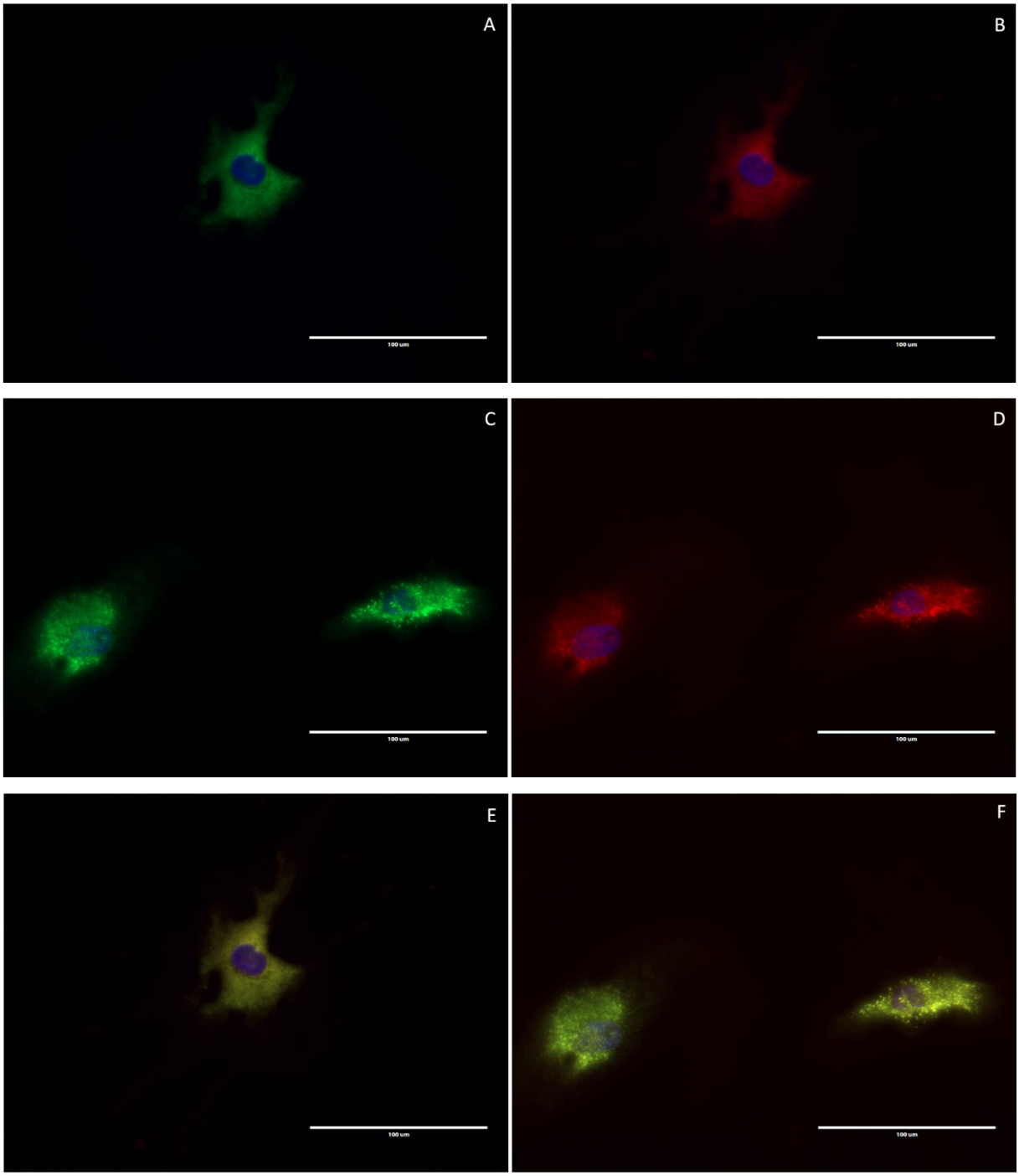

***Figure 15**: Localization of FUBP3 (red) and G3BP1 (green) in BM-MSC*

AB: control; CD: stress group; E and F merged channels for control (E) and treatment (F); Scale bar 100 µm.

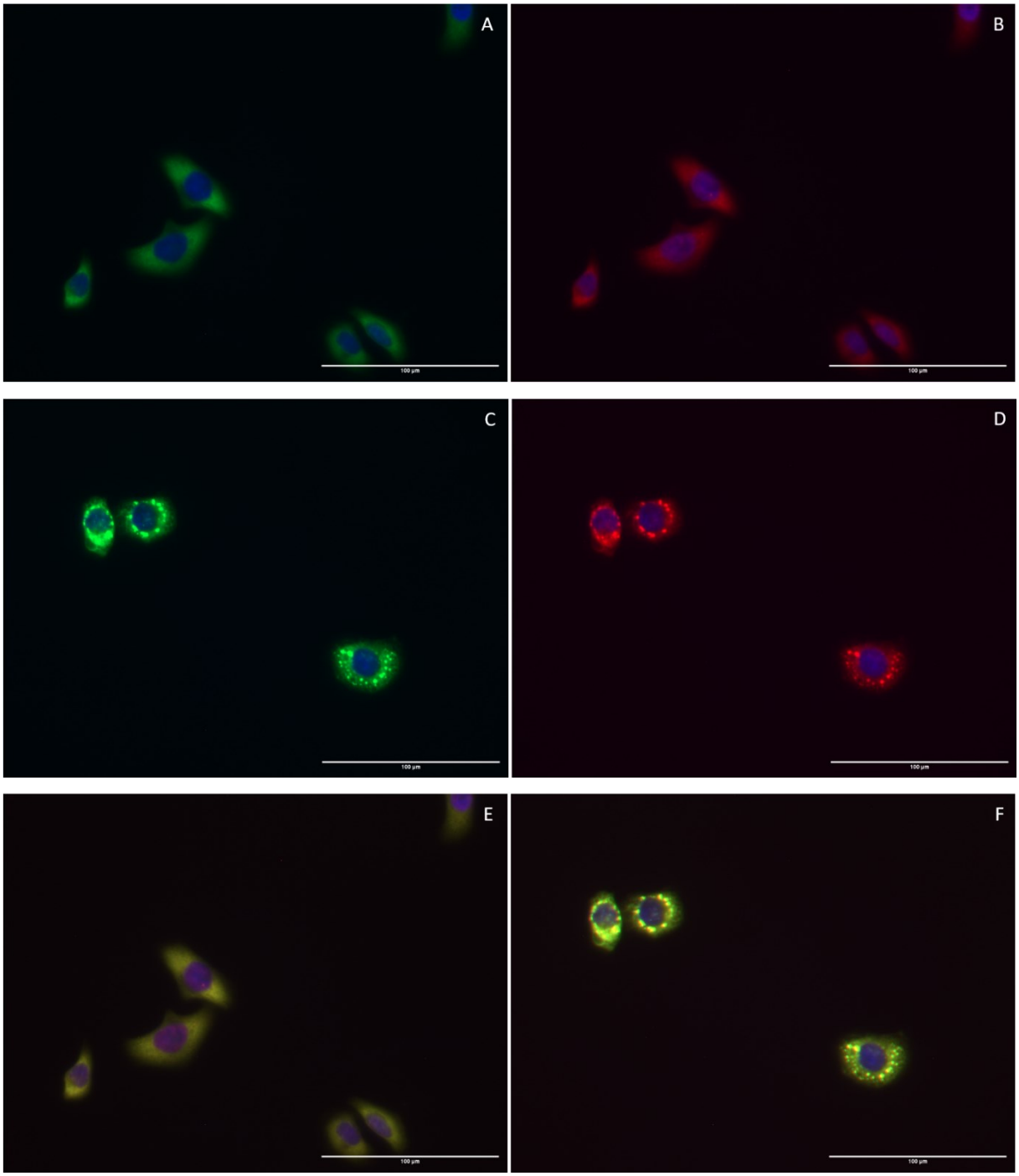

***Figure 16**: Localization of FUBP3 (red) and G3BP1 (green) in HeLa cells*

AB: control; CD: stress group; E and F merged channels for control (E) and treatment (F)

Scale bar 100 µm.

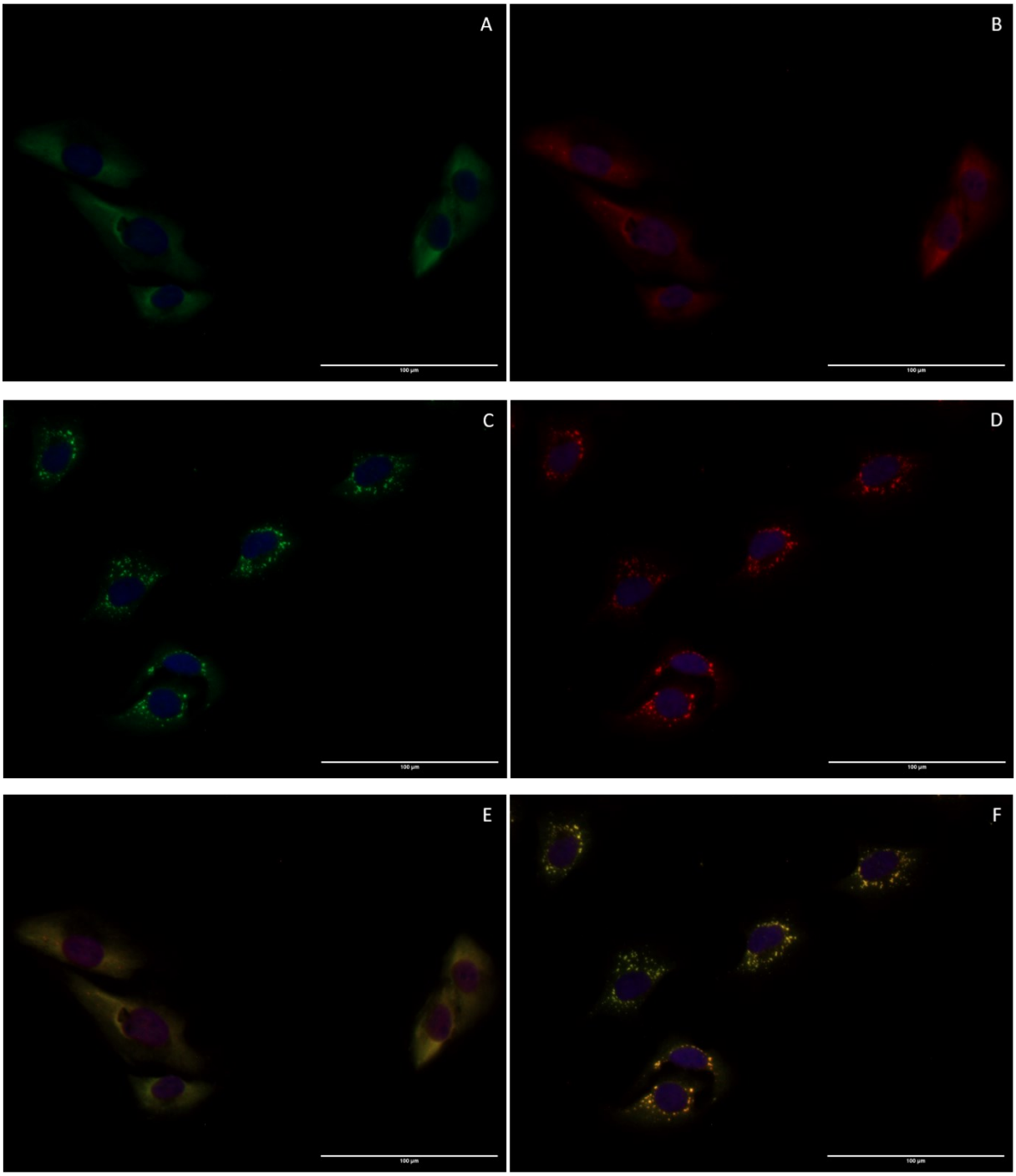

***Figure 17**: Localization of FUBP3 (red) and G3BP1 (green) in HOS cells*

AB: control; CD: stress group; E and F merged channels for control (E) and treatment (F)

Scale bar 100 µm.

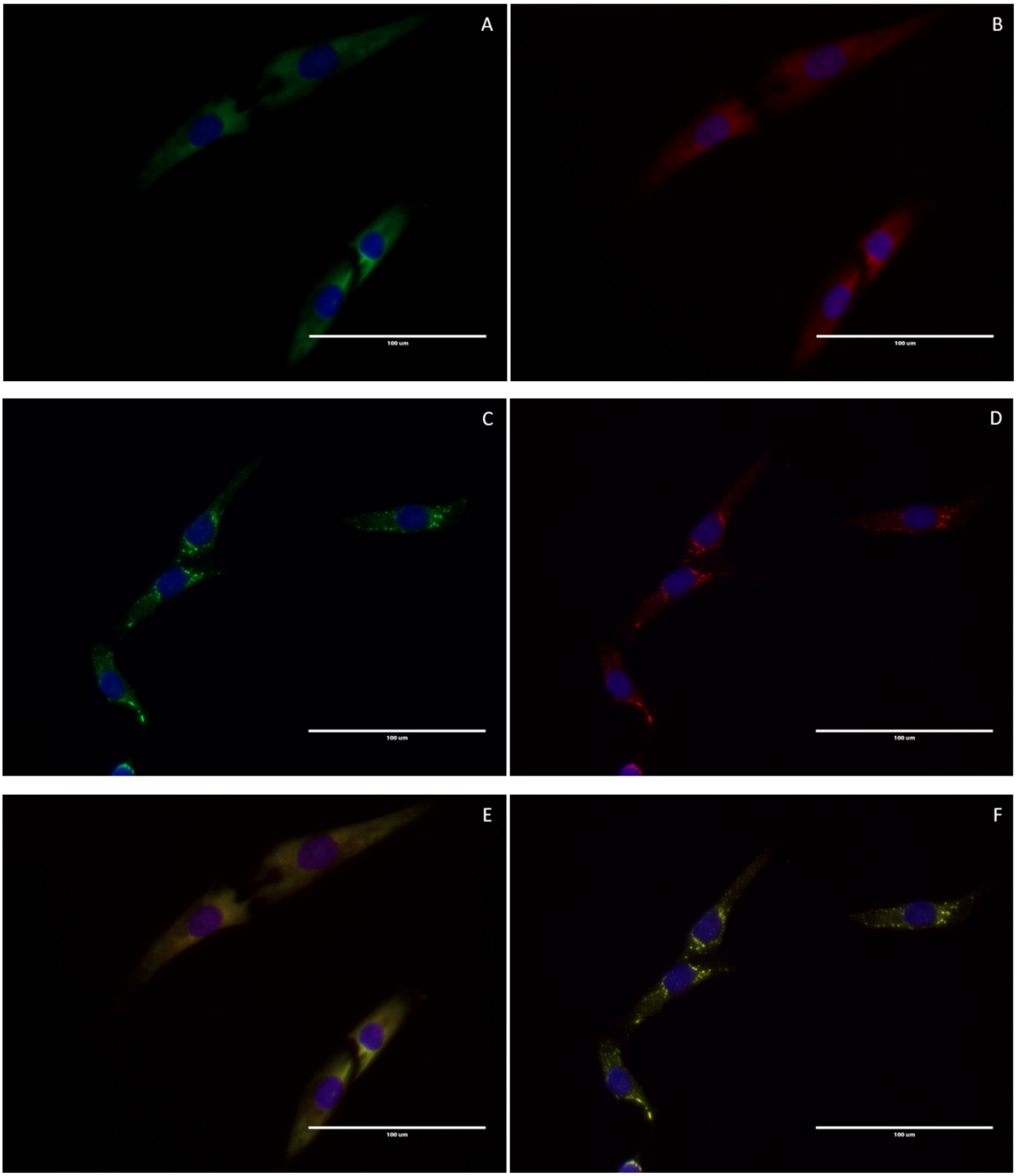

***Figure 18**: Localization of FUBP3 (red) and G3BP1 (green) in MG-63 cells*

AB: control; CD: stress group; E and F merged channels for control (E) and treatment (F)

Scale bar 100 µm.

6.2.4. Confirmation of FUBP3 knockout in MG-63 by immunofluorescence

The human osteosarcoma cell line MG-63 was chosen for qPCR investigation of the FUBP3 deficiency effect on the transcription of certain genes. In spite of that, FUBP3 knockout cells were acquired.

Wild-type MG-63 and FUBP3 knockouts were stained for comparison. In wt MG-63, the FUBP3 expression levels are comparable to other cell lines we used for the purposes of this thesis.

In wt MG-63 the FUBP3 localized in the cytoplasm and a weak signal could be found in the nucleus as well. Compared, the ko MG-63 stained for FUBP3 neither in the nucleus nor the cytoplasm of the cells. (Figure 19)

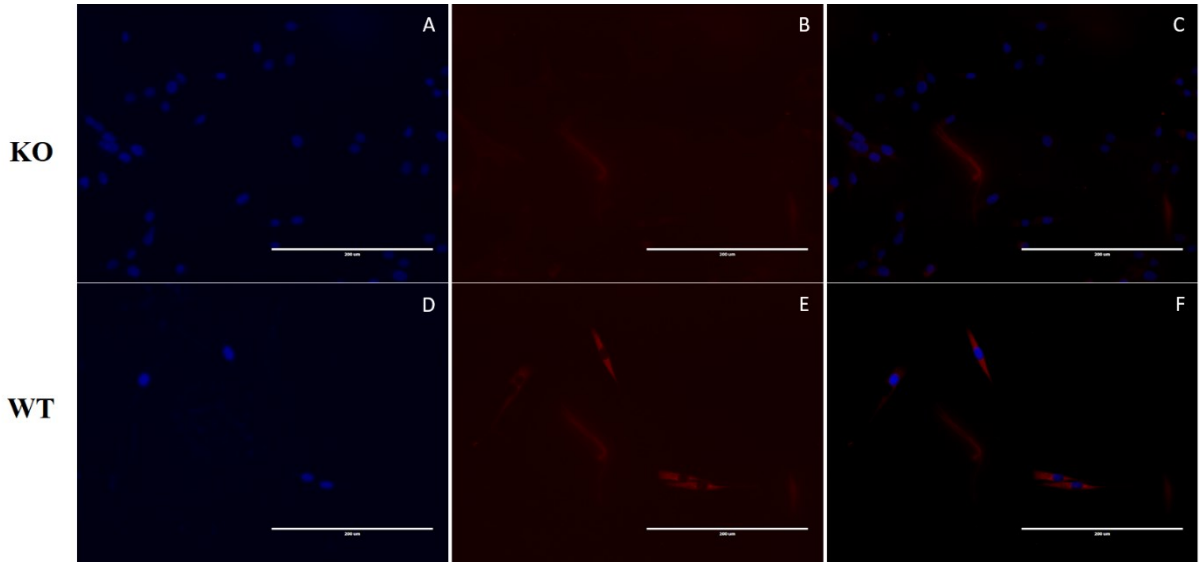

***Figure 19**: Staining of FUBP3 ko (**A-C**) and wt MG-63 cells (**D-F**); DAPI stained nuclei in blue colour; FUBP3 in red colour; left column DAPI channel – only nuclei can be seen; middle column – RFP channel to show FUBP3; right column merged DAPI and RFP; Scale bar 200 µm.*

6.3. qPCR of investigated genes in MG-63 wt and FUBP3 ko cells

For comparison of gene expression affected by FUBP3, the MG-63 wild type and FUBP3 knockout cells were chosen. The qPCR analysis was carried out once for reasons of time.

Fold change of expression was calculated using the Livak Method ($2^{-\Delta\Delta Ct}$). Certain results were not taken into account, based on the results of melting temperature measurement. Specifically, FGF, MPP7(2) and MPP7(3). For TMEM64, a second set of primers was acquired to minimise doubts.

As seen in Figure 20, TMEM64 is markedly upregulated in FUBP3 knockout cells, with fold change ranging from 1.89 to 3.16. Secondly, COL1A1 is also markedly upregulated (fold change of 2.99). Higher expression (fold change above 2) in MG-63 ko cells can be also seen in PTEN and C-MYC.

Osteocalcin (OC) on the other hand shows downregulation (-2,63-fold change) in FUBP3 knockouts.

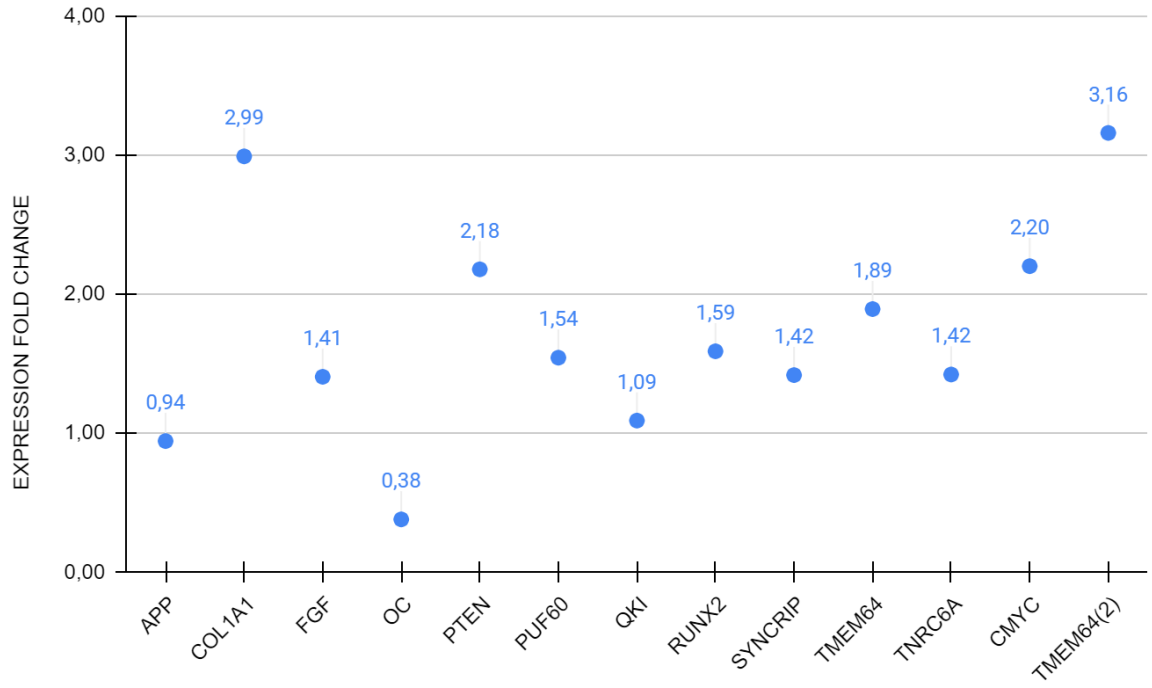

***Figure 20**: Fold change in expression of investigated genes calculated using the Livak method.*

7.Discussion

Since not much is known about the FUBP3 function, this thesis aimed to provide an overview of the FUBP3 pathway involvement and interactions. We have created a list of known interactors across databases and tested their association with osteoporosis or bone development using the OpenTargets Platform. Our results may serve as a starting point for further studies of the FUBP3 function.

Firstly, to comment on FUBP3's cellular localization, as previously observed by (Kunrt, 2020), FUBP3 predominantly localizes to the cytoplasm as opposed to the rest of FUSE binding proteins. Cytoplasmatic localisation is in line with the outcomes of the COMPARTMENTS search (Binder et al., 2014).

To our best knowledge, no paper concerning itself with the interactome of FUBP3 has been published. In this way, this thesis is unique in gathering data across various databases. However, the process through which individual databases collect interactions must be considered and our outcomes are to be used with caution.

The interactors gathered in the first part of this thesis were searched for an association to either bone mineral density (BMD), osteoporosis (OP), or both and based on further literature review (as presented in the Chapter 6.1.7), several hits were chosen for further qPCR expression analysis. However, some of our results were inconclusive, probably due to experimental errors and the fact the experiments were carried out only once. The validity of presented outcomes is limited by a low number of repeats. Subsequent qPCR in cells with higher passage numbers failed to reproduce our results. That may be the influence of further passage on the cell resulting in a decline in cell health, and data variability (Kwist et al., 2016).

The qPCR results for FGF are in line with the findings of Gau et al. (2011) who suggest that FUBP3 knockout does not influence FGF expression, but rather that FUBP3 regulates FGF protein levels post-translationally. It is also the first study to report the RNA binding properties of FUBP3.

With the above mentioned in mind, we need to add that also PUF60, QKI, RUNX2, TNRC6A or SYNCRIP and others might be furtherly regulated by FUBP3. The presented results only show that FUBP3 knockout does not influence their expression.

The higher expression of collagen type I alpha 1 chain (COL1A1) in FUBP3 knockout cells we report, is supported by evidence proposed by Han and colleagues (2022) who show that polymorphism in FUBP3 does affect protein levels of COL1A1 which are related to BMD. Furthermore, mutations in the COL1A1 gene are linked to rare monogenous forms of osteoporosis (Mäkitie et al., 2019).

As already described in chapter 6.1.7., Transmembrane protein 64 is a regulator of RANKL-mediated osteoclastogenesis. In our results, we report higher expression of TMEM64 in FUBP3 KO cells. Overexpression of TMEM64 is connected to inhibition of osteogenesis and TMEM64 knockout showed an increase in osteoblast differentiation (Jeong et al., 2015). Conversely, lower levels of TMEM64 in OP patients have been reported by Dera and colleagues (2019), who argue TMEM64 could serve as a potential OP marker. The above-mentioned seems counter-intuitive and needs further research. Altogether we can say FUBP3 control of TMEM64 levels might influence bone biology processes. Further experiments regarding the interaction between TMEM64 and FUBP3 are needed to elucidate their relationship and the role they play in the pathogenesis of OP.

We also report lower expression of osteocalcin in FUBP3 knockouts. Osteocalcin is a diagnostic marker for post-menopausal OP, and a negative correlation between serum levels of OC and BMD has been reported (Singh et al., 2015). Regulation of OC levels might also contribute to pathological processes regarding bone and other diseases.

Among interactors of FUBP3 are also well-known constituents of cytoplasmic condensates, e.g. G3BP, PABPC, TIA of stress granules or CCR4-NOT deadenylase complex of processing bodies. (Youn et al., 2019) FUBP3 has been previously recognized by mass spectroscopy as an SG component. (Jain et al., 2016) We aimed to show, whether FUBP3 co-localizes with stress granule markers. We have successfully shown co-localization with G3BP1 and PABPC1 in multiple cell lines, including bone-relevant osteosarcoma cells. Our results confirm outcomes published by Youn et al. (2018) that also claim, that FUBP3 is an SG constituent. However, the role of SGs and whether FUBP3 might be crucial for SGs formation is still to be studied. Previous experiments showed that other members of the FUBP family FUBP1 and FUBP2 interact with TIA-1 – another SG component – and that FUBP1/2 migrate from the nucleus to cytoplasmic stress granules.

8.Conclusion

We have successfully shown that a number of FUBP3 interactors are also associated with osteoporosis. We have explored the possibility that FUBP3 knockout affects the gene expression of its several interaction counterparts. And lastly, we have shown that FUBP3 co-localizes with stress granule markers and conclude FUBP3 is a constituent of said stress granules. Our results offer a launch pad for deeper studies of FUBP3 interactions and cellular processes under its influence. The signal of presented qPCR results is to be further explored. However, it already proposes a clue to the role FUBP3 plays in bone biology.

9. References

Allantaz, F., Cheng, D. T., Bergauer, T., Ravindran, P., Rossier, M. F., Ebeling, M., Badi, L., Reis, B., Bitter, H., D'Asaro, M., Chiappe, A., Sridhar, S., Pacheco, G. D., Burczynski, M. E., Hochstrasser, D., Vonderscher, J., & Matthes, T. (2012). Expression profiling of human immune cell subsets identifies miRNA-mRNA regulatory relationships correlated with cell type specific expression. *PloS One*, *7*(1). https://doi.org/10.1371/JOURNAL.PONE.0029979

Almeida, M., Han, L., Martin-Millan, M., Plotkin, L. I., Stewart, S. A., Roberson, P. K., Kousteni, S., O'Brien, C. A., Bellido, T., Parfitt, A. M., Weinstein, R. S., Jilka, R. L., & Manolagas, S. C. (2007). Skeletal Involution by Age-associated Oxidative Stress and Its Acceleration by Loss of Sex Steroids. *The Journal of Biological Chemistry*, *282*(37), 27285. https://doi.org/10.1074/JBC.M702810200

Anderson, P., & Kedersha, N. (2008). Stress granules: the Tao of RNA triage. *Trends in Biochemical Sciences*, *33*(3), 141–150. https://doi.org/10.1016/j.tibs.2007.12.003

Anderson, P., Kedersha, N., & Ivanov, P. (2015). Stress granules, P-bodies and cancer. *Biochimica et Biophysica Acta - Gene Regulatory Mechanisms*, *1849*(7), 861–870. https://doi.org/10.1016/J.BBAGRM.2014.11.009

Bastian, F. B., Roux, J., Niknejad, A., Comte, A., Fonseca Costa, S. S., de Farias, T. M., Moretti, S., Parmentier, G., de Laval, V. R., Rosikiewicz, M., Wollbrett, J., Echchiki, A., Escoriza, A., Gharib, W. H., Gonzales-Porta, M., Jarosz, Y., Laurenczy, B., Moret, P., Person, E., … Robinson-Rechavi, M. (2021). The Bgee suite: integrated curated expression atlas and comparative transcriptomics in animals. *Nucleic Acids Research*, *49*(D1), D831–D847. https://doi.org/10.1093/nar/gkaa793

Becnel, L. B., Ochsner, S. A., Darlington, Y. F., McOwiti, A., Kankanamge, W. H., Dehart, M., Naumov, A., & McKenna, N. J. (2017). Discovering relationships between nuclear receptor signaling pathways, genes, and tissues in Transcriptomine. *Science Signaling*, *10*(476). https://doi.org/10.1126/SCISIGNAL.AAH6275

Binder, J. X., Pletscher-Frankild, S., Tsafou, K., Stolte, C., O'Donoghue, S. I., Schneider, R., & Jensen, L. J. (2014). COMPARTMENTS: unification and visualization of protein subcellular localization evidence. *Database*, *2014*(0), bau012–bau012. https://doi.org/10.1093/database/bau012

Buck, D. W., & Dumanian, G. A. (2012). Bone biology and physiology: Part I. The fundamentals. *Plastic and Reconstructive Surgery*, *129*(6), 1314–1320. https://doi.org/10.1097/PRS.0B013E31824ECA94

Canalis, E. (2008). Notch Signaling in Osteoblasts. *Science Signaling*, *1*(17). https://doi.org/10.1126/STKE.117PE17

Chellaiah, M. A., Soga, N., Swanson, S., McAllister, S., Alvarez, U., Wang, D., Dowdy, S. F., & Hruska, K. A. (2000). Rho-A is critical for osteoclast podosome organization, motility, and bone resorption. *The Journal of Biological Chemistry*, *275*(16), 11993–12002. https://doi.org/10.1074/JBC.275.16.11993

Chen, X., Wang, Z., Duan, N., Zhu, G., Schwarz, E. M., & Xie, C. (2018). Osteoblast–osteoclast interactions. *Connective Tissue Research*, *59*(2), 99–107. https://doi.org/10.1080/03008207.2017.1290085

Clark, G. R., & Duncan, E. L. (2015). The genetics of osteoporosis. *British Medical Bulletin*, *113*(1), 73–81. https://doi.org/10.1093/BMB/LDU042

Consortium, T. U. (2021). UniProt: the universal protein knowledgebase in 2021. *Nucleic Acids Research*, *49*(D1), D480–D489. https://doi.org/10.1093/nar/gkaa1100

Datta, H. K., Ng, W. F., Walker, J. A., Tuck, S. P., & Varanasi, S. S. (2008). The cell biology of bone metabolism. *Journal of Clinical Pathology*, *61*(5), 577–587. https://doi.org/10.1136/JCP.2007.048868

Denny, J. C., Bastarache, L., Ritchie, M. D., Carroll, R. J., Zink, R., Mosley, J. D., Field, J. R., Pulley, J. M., Ramirez, A. H., Bowton, E., Basford, M. A., Carrell, D. S., Peissig, P. L., Kho, A. N., Pacheco, J. A., Rasmussen, L. V., Crosslin, D. R., Crane, P. K., Pathak, J., … Roden, D. M. (2013). Systematic comparison of phenome-wide association study of electronic medical record data and genome-wide association study data. *Nature Biotechnology*, *31*(12), 1102–1110. https://doi.org/10.1038/NBT.2749

Dera, A. A., Ranganath, L., Barraclough, R., Vinjamuri, S., Hamill, S., Mandourah, A. Y., & Barraclough, D. L. (2019). Altered Levels of mRNAs for Calcium-Binding/Associated Proteins, Annexin A1, S100A4, and TMEM64, in Peripheral Blood Mononuclear Cells Are Associated with Osteoporosis. *Disease Markers*, *2019*. https://doi.org/10.1155/2019/3189520

Domazetovic, V., G, M., T, I., ML, B., & MT, V. (2017). Oxidative stress in bone remodeling: role of antioxidants. *Clinical Cases in Mineral and Bone Metabolism : The Official Journal of the Italian Society of Osteoporosis, Mineral Metabolism, and Skeletal Diseases*, *14*(2), 209. https://doi.org/10.11138/CCMBM/2017.14.1.209

Duncan, E. L., & Brown, M. A. (2010). Clinical review 2: Genetic determinants of bone density and fracture risk--state of the art and future directions. *The Journal of Clinical Endocrinology and Metabolism*, *95*(6), 2576–2587. https://doi.org/10.1210/JC.2009-2406

Estrada, K., Styrkarsdottir, U., Evangelou, E., Hsu, Y. H., Duncan, E. L., Ntzani, E. E., Oei, L., Albagha, O. M. E., Amin, N., Kemp, J. P., Koller, D. L., Li, G., Liu, C. T., Minster, R. L., Moayyeri, A., Vandenput, L., Willner, D., Xiao, S. M., Yerges-Armstrong, L. M., … Rivadeneira, F. (2012). Genome-wide meta-analysis identifies 56 bone mineral density loci and reveals 14 loci associated with risk of fracture. *Nature Genetics 2012 44:5*, *44*(5), 491–501. https://doi.org/10.1038/ng.2249

Florencio-Silva, R., Sasso, G. R. D. S., Sasso-Cerri, E., Simões, M. J., & Cerri, P. S. (2015). Biology of Bone Tissue: Structure, Function, and Factors That Influence Bone Cells. *BioMed Research International*, *2015*. https://doi.org/10.1155/2015/421746

Foster, L. J., Zeemann, P. A., Li, C., Mann, M., Jensen, O. N., Kassem, M., & Sci, D. (2005). Differential Expression Profiling of Membrane Proteins by Quantitative Proteomics in a Human Mesenchymal Stem Cell Line Undergoing Osteoblast Differentiation. *Stem Cells*, *23*, 1367–1377. https://doi.org/10.1634/stemcells.2004

Gau, B. H., Chen, T. M., Shih, Y. H. J., & Sun, H. S. (2011). FUBP3 interacts with FGF9 3' microsatellite and positively regulates FGF9 translation. *Nucleic Acids Research*, *39*(9), 3582–3593. https://doi.org/10.1093/NAR/GKQ1295

Halstead, J. M., Lin, Y. Q., Durraine, L., Hamilton, R. S., Ball, G., Neely, G. G., Bellen, H. J., & Davis, I. (2014). Syncrip/hnRNP Q influences synaptic transmission and regulates BMP signaling at the Drosophila neuromuscular synapse. *Biology Open*, *3*(9), 839–849. https://doi.org/10.1242/BIO.20149027

Han, L., Wu, J., Wang, M., Zhang, Z., Hua, D., Lei, S., & Mo, X. (2022). RNA Modification-Related Genetic Variants in Genomic Loci Associated with Bone Mineral Density and Fracture. *Genes*, *13*(10). https://doi.org/10.3390/GENES13101892/S1

Han, Y., Liu, C., Lei, M., Sun, S., Zheng, W., Niu, Y., & Xia, X. (2019). LncRNA TUG1 was upregulated in osteoporosis and regulates the proliferation and apoptosis of osteoclasts. *Journal of Orthopaedic Surgery and Research*, *14*(1), 416–416. https://doi.org/10.1186/S13018-019-1430-4

Harvey, N., Dennison, E., & Cooper, C. (2010). Osteoporosis: impact on health and economics. *Nature Reviews Rheumatology 2010 6:2*, *6*(2), 99–105. https://doi.org/10.1038/nrrheum.2009.260

Hein, M. Y., Hubner, N. C., Poser, I., Cox, J., Nagaraj, N., Toyoda, Y., Gak, I. A., Weisswange, I., Mansfeld, J., Buchholz, F., Hyman, A. A., & Mann, M. (2015). A human interactome in three quantitative dimensions organized by stoichiometries and abundances. *Cell*, *163*(3), 712–723. https://doi.org/10.1016/J.CELL.2015.09.053

Hendrickx, G., Boudin, E., & Van Hul, W. (2015). A look behind the scenes: the risk and pathogenesis of primary osteoporosis. *Nature Reviews Rheumatology 2015 11:8*, *11*(8), 462–474. https://doi.org/10.1038/nrrheum.2015.48

Hsu, Y. H., & Kiel, D. P. (2012). Genome-Wide Association Studies of Skeletal Phenotypes: What We Have Learned and Where We Are Headed. *The Journal of Clinical Endocrinology & Metabolism*, *97*(10), E1958–E1977. https://doi.org/10.1210/JC.2012-1890

Hubel, P., Urban, C., Bergant, V., Schneider, W. M., Knauer, B., Stukalov, A., Scaturro, P., Mann, A., Brunotte, L., Hoffmann, H. H., Schoggins, J. W., Schwemmle, M., Mann, M., Rice, C. M., & Pichlmair, A. (2019). A protein-interaction network of interferon-stimulated genes extends the innate immune system landscape. *Nature Immunology*, *20*(4), 493–502. https://doi.org/10.1038/S41590-019-0323-3

Huh, Y. J., Kim, J. M., Kim, H., Song, H., So, H., Lee, S. Y., Kwon, S. B., Kim, H. J., Kim, H. H., Lee, S. H., Choi, Y., Chung, S. C., Jeong, D. W., & Min, B. M. (2006). Regulation of osteoclast differentiation by the redox-dependent modulation of nuclear import of transcription factors. *Cell Death and Differentiation*, *13*(7), 1138–1146. https://doi.org/10.1038/SJ.CDD.4401793

Humtsoe, J. O., Liu, M., Malik, A. B., & Wary, K. K. (2010). Lipid phosphate phosphatase 3 stabilization of beta-catenin induces endothelial cell migration and formation of branching point structures. *Molecular and Cellular Biology*, *30*(7), 1593–1606. https://doi.org/10.1128/MCB.00038-09

Jain, S., Wheeler, J. R., Walters, R. W., Agrawal, A., Barsic, A., & Parker, R. (2016). ATPase-Modulated Stress Granules Contain a Diverse Proteome and Substructure. *Cell*, *164*(3), 487–498. https://doi.org/10.1016/j.cell.2015.12.038

Jassal, B., Matthews, L., Viteri, G., Gong, C., Lorente, P., Fabregat, A., Sidiropoulos, K., Cook, J., Gillespie, M., Haw, R., Loney, F., May, B., Milacic, M., Rothfels, K., Sevilla, C., Shamovsky, V., Shorser, S., Varusai, T., Weiser, J., … D'Eustachio, P. (2020). The reactome pathway knowledgebase. *Nucleic Acids Research*, *48*(D1), D498–D503. https://doi.org/10.1093/nar/gkz1031

Jeong, B. C., Kim, T. S., Kim, H. S., Lee, S. H., & Choi, Y. (2015). Transmembrane protein 64 reciprocally regulates osteoblast and adipocyte differentiation by modulating Wnt/β-catenin signaling. *Bone*, *78*, 165–173. https://doi.org/10.1016/J.BONE.2015.05.009

Johnson, M. L., & Rajamannan, N. (2006). Diseases of Wnt signaling. *Reviews in Endocrine and Metabolic Disorders 2006 7:1*, *7*(1), 41–49. https://doi.org/10.1007/S11154-006-9003-3

Kanehisa, M., Furumichi, M., Sato, Y., Ishiguro-Watanabe, M., & Tanabe, M. (2021). KEGG: integrating viruses and cellular organisms. *Nucleic Acids Research*, *49*(D1), D545–D551. https://doi.org/10.1093/nar/gkaa970

Kanis, J. A. (2002). Osteoporosis III: Diagnosis of osteoporosis and assessment of fracture risk. *Lancet*, *359*(9321), 1929–1936. https://doi.org/10.1016/S0140-6736(02)08761-5

Kedersha, N. L., Gupta, M., Li, W., Miller, I., & Anderson, P. (1999). RNA-Binding Proteins Tia-1 and Tiar Link the Phosphorylation of Eif-2α to the Assembly of Mammalian Stress Granules. *Journal of Cell Biology*, *147*(7), 1431–1442. https://doi.org/10.1083/JCB.147.7.1431

Kemp, J. P., Morris, J. A., Medina-Gomez, C., Forgetta, V., Warrington, N. M., Youlten, S. E., Zheng, J., Gregson, C. L., Grundberg, E., Trajanoska, K., Logan, J. G., Pollard, A. S., Sparkes, P. C., Ghirardello, E. J., Allen, R., Leitch, V. D., Butterfield, N. C., Komla-Ebri, D., Adoum, A. T., … Evans, D. M. (2017). Identification of 153 new loci associated with heel bone mineral density and functional involvement of GPC6 in osteoporosis. *Nature Genetics*, *49*(10), 1468–1475. https://doi.org/10.1038/NG.3949

Kichaev, G., Bhatia, G., Loh, P. R., Gazal, S., Burch, K., Freund, M. K., Schoech, A., Pasaniuc, B., & Price, A. L. (2018). Leveraging Polygenic Functional Enrichment to Improve GWAS Power. *American Journal of Human Genetics*, *104*(1), 65–75. https://doi.org/10.1016/J.AJHG.2018.11.008

Kim, H., Kim, T., Jeong, B. C., Cho, I. T., Han, D., Takegahara, N., Negishi-Koga, T., Takayanagi, H., Lee, J. H., Sul, J. Y., Prasad, V., Lee, S. H., & Choi, Y. (2013). Tmem64 modulates calcium signaling during RANKL-mediated osteoclast differentiation. *Cell Metabolism*, *17*(2), 249–260. https://doi.org/10.1016/J.CMET.2013.01.002

Kim, S. K. (2018). Identification of 613 new loci associated with heel bone mineral density and a polygenic risk score for bone mineral density, osteoporosis and fracture. *Plos One*, *13*(7), e0200785–e0200785. https://doi.org/10.1371/JOURNAL.PONE.0200785

Kimball, J. S., Johnson, J. P., & Carlson, D. A. (2021). Oxidative Stress and Osteoporosis. *The Journal of Bone and Joint Surgery. American Volume*, *103*(15), 1451–1461. https://doi.org/10.2106/JBJS.20.00989

Kunrt, J. (2020). *Lokalizace FUBP3 proteinu v buněčné linii lidského cervikálního karcinomu* [Univerzita Karlova, Farmaceutická fakulta v Hradci Králové]. https://dspace.cuni.cz/handle/20.500.11956/117931

Kwist, K., Bridges, W. C., & Burg, K. J. L. (2016). The effect of cell passage number on osteogenic and adipogenic characteristics of D1 cells. *Cytotechnology*, *68*(4), 1661. https://doi.org/10.1007/S10616-015-9883-8

Li, S., Liu, B., Zhang, L., & Rong, L. (2014). Amyloid beta peptide is elevated in osteoporotic bone tissues and enhances osteoclast function. *Bone*, *61*, 164–175. https://doi.org/10.1016/J.BONE.2014.01.010

Li, Y. R., King, O. D., Shorter, J., & Gitler, A. D. (2013). Stress granules as crucibles of ALS pathogenesis. *Journal of Cell Biology*, *201*(3), 361–372. https://doi.org/10.1083/JCB.201302044

Licata, L., Briganti, L., Peluso, D., Perfetto, L., Iannuccelli, M., Galeota, E., Sacco, F., Palma, A., Nardozza, A. P., Santonico, E., Castagnoli, L., & Cesareni, G. (2012). MINT, the molecular

interaction database: 2012 Update. *Nucleic Acids Research*, *40*(D1). https://doi.org/10.1093/nar/gkr930

Long, F. (2011). Building strong bones: molecular regulation of the osteoblast lineage. *Nature Reviews. Molecular Cell Biology*, *13*(1), 27–38. https://doi.org/10.1038/NRM3254

Luck, K., Jailkhani, N., Cusick, M. E., Rolland, T., Calderwood, M. A., Charloteaux, B., & Vidal, M. (2016). Interactomes – Scaffolds of Cellular Systems. In R. A. Bradshaw & P. D. Stahl (Eds.), *Encyclopedia of Cell Biology* (pp. 187–198). Academic Press. https://doi.org/https://doi.org/10.1016/B978-0-12-394447-4.40037-4

Mäkitie, R. E., Costantini, A., Kämpe, A., Alm, J. J., & Mäkitie, O. (2019). New Insights Into Monogenic Causes of Osteoporosis. *Frontiers in Endocrinology*, *10*. https://doi.org/10.3389/FENDO.2019.00070

Morris, J. A., Kemp, J. P., Youlten, S. E., Laurent, L., Logan, J. G., Chai, R. C., Vulpescu, N. A., Forgetta, V., Kleinman, A., Mohanty, S. T., Sergio, C. M., Quinn, J., Nguyen-Yamamoto, L., Luco, A. L., Vijay, J., Simon, M. M., Pramatarova, A., Medina-Gomez, C., Trajanoska, K., … Richards, J. B. (2018). An atlas of genetic influences on osteoporosis in humans and mice. *Nature Genetics*, *51*(2), 258–266. https://doi.org/10.1038/S41588-018-0302-X

Ochoa, D., Hercules, A., Carmona, M., Suveges, D., Gonzalez-Uriarte, A., Malangone, C., Miranda, A., Fumis, L., Carvalho-Silva, D., Spitzer, M., Baker, J., Ferrer, J., Raies, A., Razuvayevskaya, O., Faulconbridge, A., Petsalaki, E., Mutowo, P., Machlitt-Northen, S., Peat, G., … McDonagh, E. M. (2021). Open Targets Platform: supporting systematic drug-target identification and prioritisation. *Nucleic Acids Research*, *49*(D1), D1302–D1310. https://doi.org/10.1093/nar/gkaa1027

Oláh, J., Vincze, O., Virók, D., Simon, D., Bozsó, Z., Tokési, N., Horváth, I., Hlavanda, E., Kovács, J., Magyar, A., Szucs, M., Orosz, F., Penke, B., & Ovádi, J. (2011). Interactions of pathological hallmark proteins: tubulin polymerization promoting protein/p25, beta-amyloid, and alpha-synuclein. *The Journal of Biological Chemistry*, *286*(39), 34088–34100. https://doi.org/10.1074/JBC.M111.243907

Orchard, S., Ammari, M., Aranda, B., Breuza, L., Briganti, L., Broackes-Carter, F., Campbell, N. H., Chavali, G., Chen, C., Del-Toro, N., Duesbury, M., Dumousseau, M., Galeota, E., Hinz, U., Iannuccelli, M., Jagannathan, S., Jimenez, R., Khadake, J., Lagreid, A., … Hermjakob, H. (2014). The MIntAct project - IntAct as a common curation platform for 11 molecular interaction databases. *Nucleic Acids Research*, *42*(D1), D358-63. https://doi.org/10.1093/nar/gkt1115

Oughtred, R., Rust, J., Chang, C., Breitkreutz, B. J., Stark, C., Willems, A., Boucher, L., Leung, G., Kolas, N., Zhang, F., Dolma, S., Coulombe-Huntington, J., Chatr-aryamontri, A., Dolinski, K., & Tyers, M. (2021). The BioGRID database: A comprehensive biomedical resource of curated protein, genetic, and chemical interactions. *Protein Science*, *30*(1), 187–200. https://doi.org/10.1002/pro.3978

Pakos-Zebrucka, K., Koryga, I., Mnich, K., Ljujic, M., Samali, A., & Gorman, A. M. (2016). The integrated stress response. *EMBO Reports*, *17*(10), 1374–1395. https://doi.org/10.15252/EMBR.201642195

Piñero, J., Ramírez-Anguita, J. M., Saüch-Pitarch, J., Ronzano, F., Centeno, E., Sanz, F., & Furlong, L. I. (2020). The DisGeNET knowledge platform for disease genomics: 2019 update. *Nucleic Acids Research*, *48*(D1), D845–D855. https://doi.org/10.1093/nar/gkz1021

Rodan, G. A. (1992). Introduction to bone biology. *Bone*, *13*, S3–S6. https://doi.org/10.1016/S8756-3282(09)80003-3

Rodchenkov, I., Babur, O., Luna, A., Aksoy, B. A., Wong, J. V., Fong, D., Franz, M., Siper, M. C., Cheung, M., Wrana, M., Mistry, H., Mosier, L., Dlin, J., Wen, Q., O'Callaghan, C., Li, W., Elder, G., Smith, P. T., Dallago, C., … Sander, C. (2020). Pathway Commons 2019 Update: Integration, analysis and exploration of pathway data. *Nucleic Acids Research*, *48*(D1), D489–D497. https://doi.org/10.1093/nar/gkz946

Roos, P. M. (2014). Osteoporosis in neurodegeneration. *Journal of Trace Elements in Medicine and Biology*, *28*(4), 418–421. https://doi.org/10.1016/J.JTEMB.2014.08.010

Rutkovskiy, A., Stensløkken, K.-O., & Vaage, I. J. (2016). Osteoblast Differentiation at a Glance. *Medical Science Monitor Basic Research*, *22*, 95. https://doi.org/10.12659/MSMBR.901142

Salwinski, L., Miller, C. S., Smith, A. J., Pettit, F. K., Bowie, J. U., & Eisenberg, D. (2004). The Database of Interacting Proteins: 2004 update. *Nucleic Acids Research*, *32*(DATABASE ISS.). https://doi.org/10.1093/nar/gkh086

Samaras, P., Schmidt, T., Frejno, M., Gessulat, S., Reinecke, M., Jarzab, A., Zecha, J., Mergner, J., Giansanti, P., Ehrlich, H. C., Aiche, S., Rank, J., Kienegger, H., Krcmar, H., Kuster, B., & Wilhelm, M. (2020). ProteomicsDB: A multi-omics and multi-organism resource for life science research. *Nucleic Acids Research*, *48*(D1), D1153–D1163. https://doi.org/10.1093/nar/gkz974

Shen, S. M., Zhang, C., Ge, M. K., Dong, S. S., Xia, L., He, P., Zhang, N., Ji, Y., Yang, S., Yu, Y., Zheng, J. K., Yu, J. X., Xia, Q., & Chen, G. Q. (2019). PTENα and PTENβ promote carcinogenesis through WDR5 and H3K4 trimethylation. *Nature Cell Biology*, *21*(11), 1436–1448. https://doi.org/10.1038/S41556-019-0409-Z

Singh, S., Kumar, D., & Lal, A. K. (2015). Serum Osteocalcin as a Diagnostic Biomarker for Primary Osteoporosis in Women. *Journal of Clinical and Diagnostic Research : JCDR*, *9*(8), RC04. https://doi.org/10.7860/JCDR/2015/14857.6318

Stoecklin, G., & Kedersha, N. (2013). Relationship of GW/P-Bodies with Stress Granules. *Advances in Experimental Medicine and Biology*, *768*, 197. https://doi.org/10.1007/978-1-4614-5107-5_12

Sun, M., Hu, L., Wang, S., Huang, T., Zhang, M., Yang, M., Zhen, W., Yang, D., Lu, W., Guan, M., & Peng, S. (2019). Circulating MicroRNA-19b Identified From Osteoporotic Vertebral Compression Fracture Patients Increases Bone Formation. *Journal of Bone and Mineral Research : The Official Journal of the American Society for Bone and Mineral Research*, *35*(2), 306–316. https://doi.org/10.1002/JBMR.3892

Szklarczyk, D., Gable, A. L., Lyon, D., Junge, A., Wyder, S., Huerta-Cepas, J., Simonovic, M., Doncheva, N. T., Morris, J. H., Bork, P., Jensen, L. J., & Von Mering, C. (2019). STRING v11: Protein-protein association networks with increased coverage, supporting functional discovery in genome-wide experimental datasets. *Nucleic Acids Research*, *47*(D1), D607–D613. https://doi.org/10.1093/nar/gky1131

Tang, L., Wu, M., Lu, S., Zhang, H., Shen, Y., Shen, C., Liang, H., Ge, H., Ding, X., & Wang, Z. (2021). Fgf9 Negatively Regulates Bone Mass by Inhibiting Osteogenesis and Promoting Osteoclastogenesis Via MAPK and PI3K/AKT Signaling. *Journal of Bone and Mineral Research : The Official Journal of the American Society for Bone and Mineral Research*, *36*(4), 779–791. https://doi.org/10.1002/JBMR.4230

Teitelbaum, S. L., & Ross, F. P. (2003). Genetic regulation of osteoclast development and function. *Nature Reviews Genetics 2003 4:8*, *4*(8), 638–649. https://doi.org/10.1038/nrg1122

Thul, P. J., Akesson, L., Wiking, M., Mahdessian, D., Geladaki, A., Ait Blal, H., Alm, T., Asplund, A., Björk, L., Breckels, L. M., Bäckström, A., Danielsson, F., Fagerberg, L., Fall, J., Gatto, L., Gnann, C., Hober, S., Hjelmare, M., Johansson, F., … Lundberg, E. (2017). A subcellular map of the human proteome. *Science*, *356*(6340). https://doi.org/10.1126/SCIENCE.AAL3321/SUPPL_FILE/AAL3321_THUL_SM_TABLE_S9.XLSX

Trajanoska, K., Morris, J. A., Oei, L., Zheng, H. F., Evans, D. M., Kiel, D. P., Ohlsson, C., Richards, J. B., Rivadeneira, F., Forgett, V., Leong, A., Ahmad, O. S., Laurin, C., Mokry, L. E., Ross, S., Elks, C. E., Bowden, J., Warrington, N. M., Kleinman, A., … Wilson, C. H. (2018). Assessment of the genetic and clinical determinants of fracture risk: genome wide association and mendelian randomisation study. *BMJ (Clinical Research Ed.)*, *362*. https://doi.org/10.1136/BMJ.K3225

Trajanoska, K., & Rivadeneira, F. (2019). The genetic architecture of osteoporosis and fracture risk. *Bone*, *126*, 2–10. https://doi.org/10.1016/J.BONE.2019.04.005

Uhlén, M., Fagerberg, L., Hallström, B. M., Lindskog, C., Oksvold, P., Mardinoglu, A., Sivertsson, Å., Kampf, C., Sjöstedt, E., Asplund, A., Olsson, I. M., Edlund, K., Lundberg, E., Navani, S., Szigyarto, C. A. K., Odeberg, J., Djureinovic, D., Takanen, J. O., Hober, S., … Pontén, F. (2015). Tissue-based map of the human proteome. *Science*, *347*(6220). https://doi.org/10.1126/SCIENCE.1260419/SUPPL_FILE/1260419_UHLEN.SM.PDF

Wang, C. G., Wang, L., Yang, T., Su, S. L., Hu, Y. H., & Zhong, D. (2020). Pseudogene PTENP1 sponges miR-214 to regulate the expression of PTEN to modulate osteoclast differentiation and attenuate osteoporosis. *Cytotherapy*, *22*(8), 412–423. https://doi.org/10.1016/J.JCYT.2020.04.090

Wang, T., Jiang, Y., & Xiao, L. (2013). [Expression of amyloid beta-protein in bone tissue of APP/PS1 transgenic mouse]. *Zhonghua Yi Xue Za Zhi*, *93*(1), 65–68.

Watson, E. C., & Adams, R. H. (2018). Biology of Bone: The Vasculature of the Skeletal System. *Cold Spring Harbor Perspectives in Medicine*, *8*(7), a031559–a031559. https://doi.org/10.1101/CSHPERSPECT.A031559

Watts, L., Freudenthal, B., Butterfield, N. C., Pollard, A., Komla-Ebri, D., Leitch, V., Logan, J., Mannan, N., Bassett, J. H. D., & Williams, G. R. (2020). Functional validation of the osteoporosis GWAS candidate FUBP3 in knockout mice. *Bone Reports*, *13*, 100554. https://doi.org/10.1016/J.BONR.2020.100554

Whirl-Carrillo, M., McDonagh, E. M., Hebert, J. M., Gong, L., Sangkuhl, K., Thorn, C. F., Altman, R. B., & Klein, T. E. (2012). Pharmacogenomics knowledge for personalized medicine. In *Clinical Pharmacology and Therapeutics* (Vol. 92, Issue 4, pp. 414–417). Clin Pharmacol Ther. https://doi.org/10.1038/clpt.2012.96

Xia, W. F., Jung, J. U., Shun, C., Xiong, S., Xiong, L., Shi, X. M., Mei, L., & Xiong, W. C. (2013). Swedish mutant APP suppresses osteoblast differentiation and causes osteoporotic deficit, which are ameliorated by N-acetyl-L-cysteine. *Journal of Bone and Mineral Research*, *28*(10), 2122–2135. https://doi.org/10.1002/jbmr.1954

Youn, J. Y., Dunham, W. H., Hong, S. J., Knight, J. D. R., Bashkurov, M., Chen, G. I., Bagci, H., Rathod, B., MacLeod, G., Eng, S. W. M., Angers, S., Morris, Q., Fabian, M., Côté, J. F., & Gingras, A. C. (2018). High-Density Proximity Mapping Reveals the Subcellular Organization of mRNA-Associated Granules and Bodies. *Molecular Cell*, *69*(3), 517-532.e11. https://doi.org/10.1016/j.molcel.2017.12.020

Youn, J. Y., Dyakov, B. J. A., Zhang, J., Knight, J. D. R., Vernon, R. M., Forman-Kay, J. D., & Gingras, A. C. (2019). Properties of Stress Granule and P-Body Proteomes. *Molecular Cell*, *76*(2), 286–294. https://doi.org/10.1016/j.molcel.2019.09.014

Zeng, Y., Zhang, L., Zhu, W., Xu, C., He, H., Zhou, Y., Liu, Y. Z., Tian, Q., Zhang, J. G., Deng, F. Y., Hu, H. G., Zhang, L. S., & Deng, H. W. (2016). Quantitative proteomics and integrative network analysis identified novel genes and pathways related to osteoporosis. *Journal of Proteomics*, *142*, 45–52. https://doi.org/10.1016/J.JPROT.2016.04.044

Zhao, F., Guo, L., Wang, X., & Zhang, Y. (2021). Correlation of oxidative stress-related biomarkers with postmenopausal osteoporosis: a systematic review and meta-analysis. *Archives of Osteoporosis*, *16*(1). https://doi.org/10.1007/S11657-020-00854-W

10. Supplementary materials

10.1. BioGRID interactors

ABCE1	CELF2	ELAVL1	HDAC2	MCM2	PRRC2C
AGO1	CEP85	FAM120A	HELZ	MEX3A	PSPC1
AGO2	CLEC14A	FAM120C	HIST1H4A	MEX3B	PTEN
AGO3	CNOT1	FAM195B	HNRNPA1	MKI67	PUM1
AIFM1	CNOT10	FAM98A	HNRNPA2B	MKRN2	PUM2
AKAP1	CNOT11	FANCD2	HNRNPD	MOV10	PYHIN1
Akap8	CNOT2	FBL	HNRNPH1	MRPS31	QKI
ALG13	CNOT3	FMR1	HNRNPUL1	MYC	R3HDM1
ANKRD17	COPS5	FN1	HULC	MYO9A	R3HDM2
APP	CPEB4	FOXA1	IGF2BP1	NDUFS4	RAB10
ARF4	CPSF6	FOXA3	IGF2BP2	NQO1	RAVER1
ARHGAP40	CPSF7	FOXB1	ISG15	NR2C2	RBM12
ARHGEF19	CSDE1	FOXE1	ITGA4	NTRK1	RBM20
ARHGEF25	CSRP1	FOXF1	KCTD10	NUP62	RBM33
ARHGEF4	CTIF	FOXL2	KHSRP	NUPL2	RBM47
ATXN1	CTSD	FOXP3	KIAA0355	OBSL1	RBM6
ATXN2	CUL7	FOXQ1	KIAA0430	OTUD4	RBMS1
B9D2	DAP3	FOXS1	KIF14	PABPC1	RBMS2
Bach1	DAZAP1	FUBP1	KIF1B	PABPC4	RBPMS2
BCOR	DAZL	FUS	KIF21B	PAIP2	RC3H1
BIRC3	DDX1	FXR1	KRT17	PARP12	RC3H2
BRD4	DDX3X	FXR2	LARP4B	PATL1	RECQL4
C8orf82	DDX6	G3BP1	LATS2	PAX9	RHOA
CAND1	DPF2	G3BP2	LMBR1L	PCBP1	RNF123
CAPRIN1	DPP8	GDI1	LSM12	PCBP2	RNF2
CCAR1	DUSP14	GIGYF1	LSM14A	PDHA1	RPA1
CCDC88A	DZIP3	GLE1	LSM14B	PINK1	RPA2
CDK18	E7	GRSF1	LSM4	PLEKHA4	RPA3
CDK9	EED	GTPBP1	MATR3	PRRC2A	RQCD1
CELF1	EIF4ENIF1	HCVgp1	MAU2	PRRC2B	SAMD4B

SAV1	SMG5	TARDBP	TOP3B	VCAM1	ZC3H18
SEC16A	SMG7	TDRD3	TP53	XBP1	ZC3H7A
SECISBP2	SNRNP70	TIA1	TRIM28	XRN1	ZC3HAV1
SF1	SOS2	TIAL1	TRIM56	YLPM1	ZCCHC11
SIRT7	SSX1	TNIP2	UBAP2L	YTHDF1	ZCCHC3
SMAP2	SUZ12	TNRC6A	UNK	YTHDF2	ZFP36
SMARCAD1	SYNCRIP	TNRC6B	UPF1	YTHDF3	
SMARCC1	TANK	TNRC6C	USP54	ZBTB10	

Supplementary Table 1: List of all interactors from the BioGRID database sorted alphabetically.

10.2. Association of protein interactors to bone mineral density (BMD) or osteoporosis (OP)

Molecule	Association score to BDM	Type of association	Association score to OP	Type of association	Associated with BMD/OP
CPED1	1	genetic	N/A	N/A	BMD
DICER1	1	genetic	0,01	text mining	both
KLHL42	0,96	genetic	N/A	N/A	BMD
ZBTB10	0,91	genetic	N/A	N/A	BMD
OTUD4	0,91	genetic	N/A	N/A	BMD
SMARCAD1	0,9	genetic	N/A	N/A	BMD
QKI	0,89	genetic	0,03	text mining	both
FUBP3-1	0,86	genetic	N/A	N/A	BMD
FUBP3-2	0,86	genetic	N/A	N/A	BMD
XRN1	0,81	genetic	N/A	N/A	BMD
LIN7C	0,78	genetic	N/A	N/A	BMD
MOV10	0,77	genetic	N/A	N/A	BMD
IGF2BP2	0,77	genetic	N/A	N/A	BMD
ITGA4	0,68	genetic	N/A	N/A	BMD
KIAA0355	0,67	genetic	N/A	N/A	BMD
SYNCRIP	0,61	genetic	0,01	text mining	both
ABCE1	0,6	genetic	N/A	N/A	BMD
XBP1	0,59	genetic	N/A	N/A	BMD
FGF9	0,57	genetic	N/A	N/A	BMD
FN1	0,57	genetic	0,01	text mining	both
C17orf53	0,54	genetic	N/A	N/A	BMD

Molecule	Association score to BDM	Type of association	Association score to OP	Type of association	Associated with BMD/OP
TNRC6A	0,47	genetic	N/A	N/A	BMD
RBM6	0,46	genetic	N/A	N/A	BMD
FOXF1	0,41	genetic	N/A	N/A	BMD
CPEB4	0,41	genetic	N/A	N/A	BMD
DPP8	0,35	genetic	N/A	N/A	BMD
SAV1	0,32	genetic	N/A	N/A	BMD
HNRNPUL1	0,28	genetic	N/A	N/A	BMD
PABPC4	0,27	genetic	0,01	genetic	both
RBM33	0,22	genetic	N/A	N/A	BMD
KIF1B	0,21	genetic	N/A	N/A	BMD
GTPBP1	0,19	genetic	N/A	N/A	BMD
NQO1	0,17	genetic	N/A	N/A	BMD
TMEM57	0,15	genetic	0,01	genetic	both
LSM12	0,14	genetic	N/A	N/A	BMD
FBXO8	0,13	genetic	N/A	N/A	BMD
B9D2	0,12	genetic	N/A	N/A	BMD
PTEN	0,12	genetic	0,06	text mining	both
CTIF	0,11	genetic	N/A	N/A	BMD
MAU2	0,1	genetic	N/A	N/A	BMD
ARF4	0,09	genetic	N/A	N/A	BMD
RNF123	0,09	genetic	N/A	N/A	BMD
CDK9	0,09	genetic	0,01	text mining	both
FOXS1	0,08	genetic	N/A	N/A	BMD
HNRNPF	0,08	genetic	N/A	N/A	BMD
RHOA	0,08	genetic	0,14	genetic; text mining	both
GIGYF1	0,07	genetic	N/A	N/A	BMD
DDX6	0,05	genetic	N/A	N/A	BMD
RGS22	0,05	genetic	N/A	N/A	BMD
CNOT3	N/A	N/A	0,27	text mining; animal models	OP
METTL3	N/A	N/A	0,06	text mining	OP
TMEM64	N/A	N/A	0,06	text mining	OP
VCAM1	N/A	N/A	0,04	text mining	OP
PUM1	N/A	N/A	0,04	text mining	OP
FOXA1	N/A	N/A	0,03	text mining	OP
NR2C2	N/A	N/A	0,03	text mining	OP
HDAC2	N/A	N/A	0,03	text mining	OP
ALG13	N/A	N/A	0,03	text mining	OP
UPF1	N/A	N/A	0,03	text mining	OP
TP53	N/A	N/A	0,03	text mining	OP

Molecule	Association score to BDM	Type of association	Association score to OP	Type of association	Associated with BMD/OP
KHDRBS1	N/A	N/A	0,03	text mining	OP
APP	N/A	N/A	0,02	text mining	OP
BRD4	N/A	N/A	0,02	text mining	OP
GAPDH	N/A	N/A	0,02	text mining	OP
ATXN1	N/A	N/A	0,01	text mining	OP
MYC	N/A	N/A	0,01	text mining	OP
TANK	N/A	N/A	0,01	text mining	OP
ATXN2	N/A	N/A	0,01	genetic	OP
FMR1	N/A	N/A	0,01	text mining	OP
HNRNPL	N/A	N/A	0,01	text mining	OP
RBMS1	N/A	N/A	7,15E-05	genetic	OP
TNRC6B	N/A	N/A	6,28E-05	genetic	OP
KIF21B	N/A	N/A	3,58E-05	genetic	OP
PRRC2A	N/A	N/A	0	genetic	OP
SF1	N/A	N/A	0	genetic	OP

Supplementary Table 2: FUBP3 interactors associated with osteoporosis (OP) and/or bone mineral density (BMD). The interactors are sorted by the score of association as scored by the OpenTargets platform on a scale of 1 to 0.